AGU PUBLICATIONS

Global Biogeochemical Cycles

RESEARCH ARTICLE
10.1002/2015GB005141

Key Points:
- Biogeochemistry of oligotrophic gyres can vary on timescales from days to weeks
- A period of sustained net heterotrophy was observed during August 2012
- A low surface salinity feature propagated through the field site

Supporting Information:
- Tables S1 and S2

Correspondence to:
S. T. Wilson,
stwilson@hawaii.edu

Citation:
Wilson, S. T., et al. (2015), Short-term variability in euphotic zone biogeochemistry and primary productivity at Station ALOHA: A case study of summer 2012, *Global Biogeochem. Cycles, 29*, 1145–1164, doi:10.1002/2015GB005141.

Received 19 MAR 2015
Accepted 10 JUL 2015
Accepted article online 14 JUL 2015
Published online 13 AUG 2015

Short-term variability in euphotic zone biogeochemistry and primary productivity at Station ALOHA: A case study of summer 2012

Samuel T. Wilson[1,2], Benedetto Barone[1,2], Francois Ascani[1,3], Robert R. Bidigare[1,4], Matthew J. Church[1,2], Daniela A. del Valle[1,2], Sonya T. Dyhrman[1,5], Sara Ferrón[1,2], Jessica N. Fitzsimmons[1,6], Laurie W. Juranek[7], Zbigniew S. Kolber[1,8], Ricardo M. Letelier[1,7], Sandra Martínez-García[1,2,9], David P. Nicholson[1,10], Kelvin J. Richards[1], Yoshimi M. Rii[1,2], Mónica Rouco[1,5], Donn A. Viviani[1,2], Angelicque E. White[1,7], Jonathan P. Zehr[1,8], and David M. Karl[1,2]

[1]Daniel K. Inouye Center for Microbial Oceanography: Research and Education (C-MORE), University of Hawai'i at Manoa, Honolulu, Hawai'i, USA, [2]Department of Oceanography, University of Hawai'i at Manoa, Honolulu, Hawai'i, USA, [3]Now at Marine Science Department, University of Hawai'i at Hilo, Hilo, Hawai'i, USA, [4]Hawai'i Institute of Marine Biology, University of Hawai'i, Kaneohe, Hawai'i, USA, [5]Department of Earth and Environmental Sciences and the Lamont-Doherty Earth Observatory, Columbia University, Palisades, New York, USA, [6]Now at Department of Oceanography, Texas A&M University, College Station, USA, [7]College of Earth, Ocean, and Atmospheric Sciences, Oregon State University, Corvallis, Oregon, USA, [8]Department of Ocean Sciences, University of California, Santa Cruz, California, USA, [9]Now at Centre for Ecology and Evolution in Microbial model Systems – EEMiS, Linnaeus University, SE–39182 Kalmar, Sweden, [10]Marine Chemistry and Geochemistry Department, Woods Hole Oceanographic Institution, Woods Hole, Massachusetts, USA

Abstract Time-series observations are critical to understand the structure, function, and dynamics of marine ecosystems. The Hawaii Ocean Time-series program has maintained near-monthly sampling at Station ALOHA (22°45′N, 158°00′W) in the oligotrophic North Pacific Subtropical Gyre (NPSG) since 1988 and has identified ecosystem variability over seasonal to interannual timescales. To further extend the temporal resolution of these near-monthly time-series observations, an extensive field campaign was conducted during July–September 2012 at Station ALOHA with near-daily sampling of upper water-column biogeochemistry, phytoplankton abundance, and activity. The resulting data set provided biogeochemical measurements at high temporal resolution and documents two important events at Station ALOHA: (1) a prolonged period of low productivity when net community production in the mixed layer shifted to a net heterotrophic state and (2) detection of a distinct sea-surface salinity minimum feature which was prominent in the upper water column (0–50 m) for a period of approximately 30 days. The shipboard observations during July–September 2012 were supplemented with in situ measurements provided by Seagliders, profiling floats, and remote satellite observations that together revealed the extent of the low productivity and the sea-surface salinity minimum feature in the NPSG.

1. Introduction

Understanding ocean ecosystems requires the collection of long-term, ecological time-series data at multiple locations in the world's oceans. The Hawaii Ocean Time-series (HOT) program [*Karl and Lukas*, 1996] has been sampling Station (Stn) ALOHA, situated in the North Pacific Subtropical Gyre (NPSG) at 22°45′N, 158°00′W, since October 1988, maintaining the original research objectives to observe and interpret physical and biogeochemical variability in the NPSG ecosystem [*Church et al.,* 2013; *Karl and Church*, 2014]. The scientific rationale and foresight to situate an oceanographic time-series program in the relatively stable oligotrophic gyre ecosystem to observe changes over seasonal and decadal timescales has proven to be valuable [*Venrick*, 1995]. Near-monthly hydrographic and biogeochemical observations have documented ecosystem variability over timescales ranging from interannual, e.g., increasing oceanic CO_2 inventories [*Keeling et al.,* 2004; *Dore et al.,* 2009], climate-related biological changes [*Corno et al.,* 2007; *Bidigare et al.,* 2009] to seasonal cycles of phytoplankton productivity [*Letelier et al.,* 1996; *Quay et al.,* 2010], nitrogen fixation [*Church et al.,* 2009], and the downward flux of particulate organic matter [*Karl et al.,* 2012].

Augmentation of shipboard time-series observations with higher resolution in situ observations and experimentation has provided new insight into spatiotemporal variability in the open ocean. Recent oceanographic fieldwork in the oligotrophic NPSG has identified pelagic ecosystem variability not captured

by the monthly sampling maintained by the HOT program. Recent examples of such field-based research include characterization of phytoplankton blooms [*Fong et al.,* 2008; *Villareal et al.,* 2012], eddy-driven export of plankton biomass [*Guidi et al.,* 2012], and the vertical entrainment of nutrients into the lower regions of euphotic zone [*Johnson et al.,* 2010; *Ascani et al.,* 2013]. However, these oceanographic measurements differ from the Eulerian sampling strategy of the upper water column maintained by the HOT program, and until now, high-resolution fixed-point observations of hydrographic and biogeochemical parameters during an entire season have not been achieved. Accomplishing this goal would help resolve the connections between biological and physical variability and identify the propagation of individual features and their associated biogeochemical properties through the study site which may otherwise be misinterpreted as temporal variability [*McGillicuddy*, 2001; *Karl et al.,* 2002; *Martin*, 2003].

In summer 2012, an extensive field campaign designed to improve the temporal resolution of upper water-column hydrographic and biogeochemical measurements in the NPSG was conducted by the Center for Microbial Oceanography: Research and Education (C-MORE). The upper ocean during the summer months, which vary in definition but broadly extend from June to September, is characterized by relatively shallow mixed layers, elevated daily light flux, low nutrient inventories, and episodic phytoplankton blooms that include diatoms in conjunction with nitrogen (N_2)-fixing cyanobacteria or solely N_2-fixing microorganisms (e.g., *Trichodesmium* spp.) [*Dore et al.,* 2008; *Church et al.,* 2009; *Wilson et al.,* 2013]. It is during the summer period that an export pulse of sinking particulate material from the euphotic zone usually occurs [*Karl et al.,* 2012], indicating a transient disconnect between production and consumption mechanisms. In the oligotrophic gyres, photosynthesis and respiration are generally tightly coupled with a resulting net metabolic balance slightly in favor of autotrophy [*Williams et al.,* 2013], although net heterotrophic conditions have also been inferred [*Duarte et al.,* 2013]. The metabolic balance, in terms of oxygen (O_2) and carbon (C), is represented by the residual between gross primary production (GPP) and community respiration (CR), referred to as net community production (NCP). NCP is a small yet critical term in the global C cycle as it represents the biologically produced C available for export from the upper ocean [*Emerson*, 2014].

This paper reports the hydrographic and biogeochemical conditions of the upper water column at Stn ALOHA between July and September 2012. A striking observation during this period was the absence of any prolonged increase in phytoplankton biomass or bloom activity that is often observed during the summer time in the NPSG. Instead, anomalously low values of phytoplankton abundance and a period of net heterotrophy were recorded. In the absence of local or regional physical forcing mechanisms, we have identified several indicators of ecosystem-scale forcing that potentially contributed to this period of net heterotrophy. A separate hydrographic phenomenon, described as a "sea-surface salinity minimum," was also observed and characterized. The low salinity water was associated with anomalously low concentrations of particulate material and phytoplankton. The daily measurements collected in this study are placed within the context of the 1988–2011 time-series climatology provided by the HOT program's measurements at Stn ALOHA. Ultimately, the high-resolution Eulerian observations revealed the day-to-day biogeochemical variability of the upper water column and identified hydrographic features that impact this open ocean oligotrophic habitat.

2. Materials and Methods

2.1. Field Operations and Sampling

During 2012, a series of C-MORE-sponsored oceanographic expeditions collectively known as Hawaii Ocean Experiment: Dynamics of Light and Nutrients (HOE-DyLAN) conducted operations at Stn ALOHA onboard the R/V *Kilo Moana* (Table 1). Three major expeditions covered a period from 8–28 July (KM12-15), 5–14 August (KM12-17), and 22 August to 11 September 2012 (KM12-19). These C-MORE cruises were interspersed with monthly HOT program cruises (Table 1).

To characterize the upper water column, vertical profiles of hydrographic parameters were conducted every 4 h during the three major cruises, typically to a depth of 400 m with a deeper cast extending to 1000 m conducted at 0800 h daily. The conductivity-temperature-depth (CTD) package (SBE 911Plus, Sea-Bird) was attached to a 24 × 12 L Niskin® bottle rosette that also incorporated fluorescence, O_2, and in situ ultraviolet spectrophotometer (ISUS, version 3, Satlantic) sensors. The conductivity, chlorophyll *a* fluorescence, and O_2 sensors were calibrated using discrete measurements of salinity [*Bingham and Lukas,* 1996], fluorometric

Table 1. Oceanographic Expeditions to Stn ALOHA Between July and September 2012

Cruise ID	Project	Dates
KM12-15	C-MORE	8–28 Jul
KM12-16	HOT-244	30 Jul to 3 Aug
KM12-17	C-MORE	5–14 Aug
KM12-18	HOT-245	16–20 Aug
KM12-19	C-MORE	22 Aug to 11 Sep

analysis of chlorophyll *a* and phaeopigments [*Strickland and Parsons,* 1972], and dissolved O_2 [*Carritt and Carpenter,* 1966], respectively. The mixed layer depth (MLD) was calculated based on a seawater potential density anomaly of 0.125 from the sea surface.

During May through October 2012, a continuous traverse of a 50 km by 50 km "bowtie"-shaped formation which extended from Stn ALOHA to the northeast was maintained by Seaglider operations. Each Seaglider cycle reached a maximum depth of 800 m, lasted approximately 6 h, and extended a horizontal distance of 3–5 km between surfacing. The bowtie formation was completed approximately every 2 weeks, allowing for calibration with shipboard measurements when the Seagliders traversed through Stn ALOHA. The Seagliders were equipped with a CTD package (Sea-Bird) and sensors for O_2 (Sea-Bird SBE-43 and Aanderaa Optode 3830), fluorescence, and optical backscatter (WET Labs) [*Eriksen et al.,* 2001].

2.2. Biogeochemical Analyses

The CTD casts conducted every 4 h were sampled systematically to determine the hydrographic and biogeochemical properties of the water column. The biogeochemical properties of the water column (nutrients, particulates, and pigments) were sampled by conducting vertical profiles at least every 3 days from discrete depths of 5, 25, 45, 75, 100, 125, 150, and 175 m. The vertical profiles were supplemented by higher temporal-resolution sampling at targeted depth horizons, e.g., at 25 m within the mixed layer. To ensure consistency of measurements at Stn ALOHA, the majority of sampling and analytical protocols were identical to those employed by the HOT program (http://hahana.soest.hawaii.edu/index.html). In brief, nutrient analysis which included nitrite (NO_2^-) plus nitrate (NO_3^-) and phosphate was performed on land using a Bran+Luebbe Autoanalyzer III. $NO_2^- + NO_3^-$ was also determined using the chemiluminescence method for samples collected from 0 to 175 m as this method has an improved detection limit of 1 nmol L^{-1} [*Dore and Karl,* 1996]. Seawater samples for particulate carbon (PC) and particulate nitrogen (PN) were collected onto combusted 25 mm diameter Whatman glass fiber filters (GF/F). The filters were stored frozen until analyzed using an Exeter CE-440 CHN elemental analyzer (Exeter Analytical, UK).

Phytoplankton pigments were analyzed using high performance liquid chromatography (HPLC) as described by *Bidigare et al.* [2005]. Six diagnostic biomarker pigments representative of the major phytoplankton taxa are reported that include fucoxanthin, 19′-hexanoyloxyfucoxanthin, 19′-butanoyloxyfucoxanthin, zeaxanthin, divinylchlorophyll *a*, and monovinylchlorophyll *a*. Sample volumes consisted of 2–4 L captured onto Whatman GF/F filters, wrapped in foil, flash frozen, and stored at −80°C. Pigments were extracted in 3 mL of 100% acetone in the dark at 4°C for 12 h followed by vortexing, centrifugation, and subsequent analysis using a Varian 9012 HPLC system.

To characterize the N_2-fixing microorganisms, the *nifH* gene that encodes a subunit of the nitrogenase enzyme was quantified using quantitative polymerase chain reaction (qPCR). The groups of diazotrophs targeted included UCYN-A, *Crocosphaera* spp., *Trichodesmium* spp., and two types of heterocystous cyanobacteria that form symbioses with diatoms. Discrete seawater samples (2–4 L) were collected using the CTD rosette, filtered using a peristaltic pump onto 10 μm polyester (GE Osmotics, Minnetonka, MN) and 0.2 μm Supor (Cole Parmer, Vernon Hills, IL) filters in series, frozen in liquid nitrogen, and stored at −80°C until processed. The DNA extraction was conducted using published protocols [*Moisander et al.,* 2008] and the qPCR analyses conducted as previously described [*Goebel et al.,* 2010].

Four independent shipboard measurements of productivity were conducted during July–September, although not all measurements extended for the entire period. Productivity measurements included the assimilation of ^{14}C-labeled bicarbonate ($NaH^{14}CO_3$) into particulate matter [*Letelier et al.,* 1996], active fluorescence using fast repetition rate fluorometry (FRRF) [*Kolber and Falkowski*, 1993], and two dissolved gas measurements: triple O_2 isotope ($^{17}\Delta$) abundance to derive GPP [*Luz and Barkan*, 2000] and ratios of O_2/Argon (O_2/Ar) to derive net community production (NCP) [*Kaiser et al.,* 2005]. Seawater samples for ^{14}C

assimilation were collected predawn at 0400 h, dissolved O_2/Ar and triple O_2 isotope ($^{17}\Delta$) were collected at 0800 h, and FRRF were collected at 1600 h. Due to the diel variability in O_2 concentrations resulting from biological activity [*Hamme et al.,* 2012; *Tortell et al.,* 2014], calculation of NCP from instantaneous measurements of O_2/Ar in the early morning may result in an underestimation of NCP at Stn ALOHA by up to 20% compared to the daily mean rate [*Ferrón et al.,* 2015]. Since our samples for O_2/Ar analysis were collected at 0800 h when O_2/Ar is at its lowest value (NCP is lowest at night and instantaneous NCP is negative), our measurements represent a lower estimate of NCP.

For the measurements of ^{14}C incorporation, seawater was collected at 0400 h from a depth of 25 m into 500 mL acid-washed polycarbonate bottles in triplicate, spiked with $NaH^{14}CO_3$, and incubated on-deck over the full daylight period [*Letelier et al.,* 1996]. The on-deck incubators were screened to the light levels equivalent to a depth of 25 m in the water column using blue acrylic shielding and flow-through surface seawater to maintain temperature. Sampling protocols for ^{14}C assimilation measurements were identical for HOT and C-MORE cruises, except the sample incubations were conducted in situ during the HOT expeditions rather than in on-deck incubators. To quantify ^{14}C assimilation, seawater was filtered onto 25 mm diameter Whatman GF/F filters and placed into scintillation vials. After acidifying with 1 mL of 2 M HCl and venting for 24 h to remove inorganic ^{14}C, 10 mL of scintillation cocktail (UltimaGold LLT, PerkinElmer) was added to each vial and the radioactivity counted on a Packard liquid scintillation counter (TriCarb2770TR/LT) and quench corrected using internal protocols. Rates of ^{14}C incorporation (^{14}C-PP) are reported per day and represent the net incorporation of carbon into particulate matter during the daylight period.

FRRF measurements were conducted on the ship's underway seawater system and from vertical CTD hydrocasts conducted daily at noon. The FRRF instrument was operated with a broadband excitation source in the 430–545 nm range. The FRRF-based estimates of primary production (FRRF-PP) rates were calculated at time intervals of 15 min using the deckboard photosynthetically active radiation (PAR) data, with the light propagation along the water column based on light attenuation coefficient provided by daily measurements of a hyperspectral radiometer (Satlantic). These rates were integrated over a 24 h period using first-order interpolation to provide daily rates of FRRF-PP. The rates of FRRF-PP were calculated according to *Suggett et al.* [2003], assuming 8 mol quanta/mol O_2 and an average size of the photosynthetic unit of 500 (chlorophyll:reaction center).

The O_2/Ar measurements were conducted by filling 12 mL vials (Exetainer, Labco Ltd), preserving with mercuric chloride ($HgCl_2$), and analyzing the O_2/Ar ratios using a membrane inlet mass spectrometer (MIMS) [*Kana et al.,* 1994]. Reference measurements consisted of filtered (0.2 μm) surface seawater, and the analytical temperature for reference seawater and samples was maintained at 23°C by immersing the 1/16″ stainless steel inlet tubing inside a water bath. Gases were extracted through a semipermeable silicone membrane connected to a vacuum system and passed through a liquid N_2 U-tube bath to extract water vapor before entering a quadruple mass spectrometer (Pfeiffer HiCube).

Net community production (NCP) was calculated using two methods as described in *Hamme et al.* [2012]. The more traditional approach assumes that the water column is in steady state and that vertical mixing and lateral mixing are negligible. Therefore, the net biological production or consumption of O_2 in the mixed layer can be estimated from the gas exchange of biological O_2 [*Kaiser et al.,* 2005] as follows:

$$\mathrm{NCP} = k_w * \mathrm{O_2eq} * \Delta(\mathrm{O_2/Ar}) \quad (1)$$

where k_w is the weighted gas transfer velocity for O_2 (m d^{-1}), O_2eq is the equilibrium concentration of dissolved O_2 (mmol m^{-3}) in the mixed layer, and $\Delta(O_2/Ar)$ is the deviation of O_2/Ar from equilibrium, calculated as follows:

$$\Delta(\mathrm{O_2/Ar}) = \left[\frac{(\mathrm{O_2/Ar})_{\mathrm{sample}}}{(\mathrm{O_2/Ar})_{\mathrm{eq}}} - 1\right] \quad (2)$$

where $(O_2/Ar)_{sample}$ is the measured ratio in the sample and $(O_2/Ar)_{eq}$ is the ratio expected at saturation equilibrium, calculated using the solubility equations of *García and Gordon* [1992] for O_2 and *Hamme and Emerson* [2004] for Ar. The gas transfer velocity used in equation (1) was estimated from the wind speeds recorded at the WHOTS buoy using the wind speed parameterization and Schmidt numbers from *Wanninkhof* [2014] and a 20 day weighting algorithm following *Reuer et al.* [2007] to account for wind

Table 2. Summary of Productivity Measurements Conducted at Stn ALOHA From July Through September 2012[a]

Method	8–28 Jul	5–14 Aug	22 Aug to 11 Sep
Prior O_2/Ar-NCP	6.0 ± 3.2 (*n* = 16)	−7.6 ± 4.2 (*n* = 8)	−0.5 ± 3.1 (*n* = 16)
Real-time O_2/Ar-NCP	1.6 ± 2.6	3.9 ± 2.2	n/d
^{14}C-PP (carbon)	36.3 ± 6.5 (*n* = 16)	26.7 ± 5.1 (*n* = 7)	33.1 ± 7.4 (*n* = 16)
^{14}C-PP (O_2)	39.9 ± 7.2	29.4 ± 5.5	36.4 ± 8.2
FRRF-PP	52.5 ± 13.2 (*n* = 17)	n/d	52.7 ± 12.9 (*n* = 16)
$^{17}\Delta O_2$-GPP	n/d	n/d	90.7 ± 35.3 (*n* = 22)

[a]The values represent MLD-integrated in units of mmol O_2 m^{-2} d^{-1} (using a conversion PQ of 1.1 for ^{14}C-assimilation which are also reported in units of carbon). The mean ± 1 standard deviation are shown for each set of measurements and absence of sample collection or calculation is indicated by not determined (n/d). The dates represent the start and end of each expedition and the number of samples is indicated by (*n*).

speed variability prior to the measurement (Table S1 of the supporting information). We refer to NCP derived from equation (1) as "prior O_2/Ar-NCP" since it averages over a time period prior to the measurements. An alternative approach to calculate NCP is from the rate of change of $\Delta(O_2/Ar)$ during the expedition by fitting a linear regression to $\Delta(O_2/Ar)$ with time [*Hamme et al.,* 2012].

$$\mathrm{NCP} = k_{O2}{*}\mathrm{O_2eq}{*}\,\Delta(\mathrm{O_2/Ar}) + \mathrm{MLD}\frac{\mathrm{d}(\Delta(\mathrm{O_2/Ar}))}{\mathrm{d}t}{*}\mathrm{O_2eq} \quad (3)$$

where k_{O2} is the nonweighted gas transfer velocity for O_2, MLD is the average mixed layer depth, and the rate of change of $\Delta(O_2/Ar)$ was calculated by fitting a linear regression to the daily $\Delta(O_2/Ar)$ values. This method has previously been reported for NCP over timescales of hours to days [*Hamme et al.,* 2012; *Tortell et al.,* 2014] and is hereafter referred to as "real-time O_2/Ar-NCP," as it averages over the period of time when the measurements were taken.

Samples for triple O_2 isotope ($^{17}\Delta$) analysis were collected during the third major expedition. Measurements were made daily from a depth of 25 m at 0800 h from 23 August to 7 September and also at 4 h intervals between 31 August and 1 September. The same sampling and analytical protocols were followed as reported by *Juranek and Quay* [2005]. Samples were collected from Niskin bottles into pre-evacuated, $HgCl_2$ poisoned, 200 mL glass flasks to limit atmospheric contamination. Samples were analyzed at Oregon State University using the same mass spectrometer measurement procedure as described in *Juranek and Quay* [2005]. Rates of gross primary production ($^{17}\Delta$-GPP) were determined by the method of *Luz and Barkan* [2000] using the water-column parameters, MLD, wind speeds, and gas transfer velocity as described for determining NCP from O_2/Ar analysis (Table S1).

A comparison of the four productivity measurements is provided in Table 2 based on MLD-integrated production in units of O_2. The volumetric rates of ^{14}C-PP and FRRF-PP were converted to MLD-integrated values, assuming the 25 m sampling depth was representative of the mixed layer. The ^{14}C-PP measurements were converted to equivalent units of O_2 using a photosynthetic quotient (PQ) of 1.1 which is suitable for regenerated production in the oligotrophic gyre ecosystem [*Laws*, 1991]. To identify differences between rates of production for the separate expeditions a two-way analysis of variance and two-sample *t*-test were utilized after checking data for heterogeneity of variance.

2.3. Additional Data Sets Used

The online Global Marine Argo Atlas data set was used to help analyze Argo float data sets for sea-surface salinity in the vicinity of Stn ALOHA during July–September 2012 [*Roemmich and Gilson*, 2009]. In particular, vertical profiles of pressure, temperature, and conductivity were retrieved from three Webb Research APEX profiling floats (Float IDs #5903888, 5903273, and 5902241) that were in the vicinity of Stn ALOHA during July–September 2012. The profiles were conducted between the surface and 1000 m every 2, 5, and 10 day intervals for the three floats, respectively.

Meteorological measurements were provided by the WHOTS buoy situated at Stn ALOHA from June 2012 to July 2013 (http://uop.whoi.edu/projects/WHOTS/whotsdata.htm). Downwelling irradiance above the sea surface in the PAR spectral region was measured using a cosine sensor (LI-COR LI-192) mounted on the top deck of the R/V *Kilo Moana*. Measurements of horizontal velocity in the upper water column were obtained using a hull-mounted Acoustic Doppler Current Profiler (ADCP) (RDI Ocean Surveyor 300 kHz).

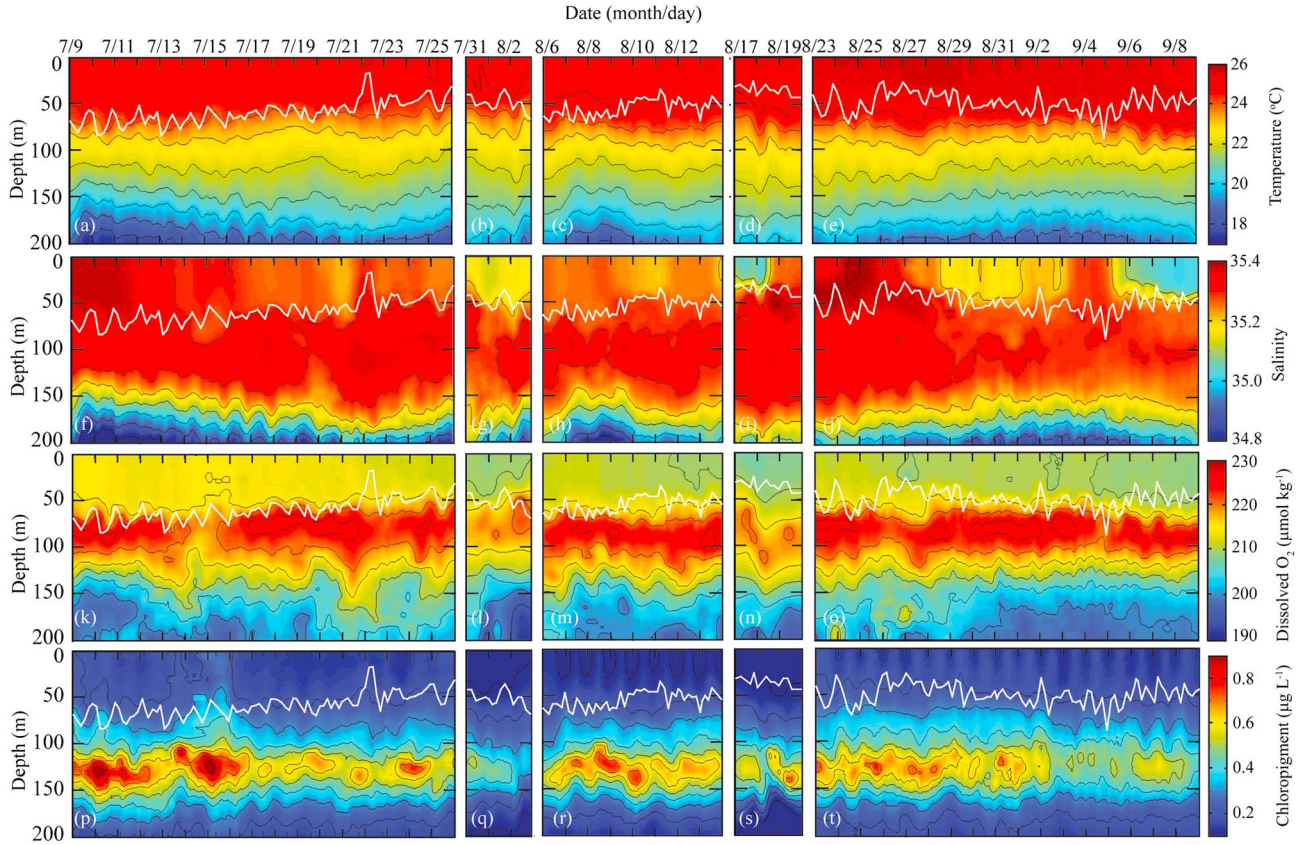

Figure 1. Upper water-column properties at Stn ALOHA from July through September 2012 showing (a–e) temperature, (f–j) salinity, (k–o) oxygen, and (p–t) chl*a* + phaeopigments. CTD profiles were conducted every 3 h during HOT cruises and every 4 h during C-MORE cruises (Table 1), and the white line represents the mixed layer depth.

To place the shipboard measurements in a wider spatial-temporal context, the surface flow within the Hawaii regional domain (15–27°N, 150–160°W) was analyzed using the Hybrid Coordinate Ocean Model (HYCOM) which is run in real time at the Naval Oceanographic Office at 1/12 degree resolution [*Chassignet et al.,* 2009]. Satellite observations of regional ocean color (2002–2012, 8 day averages) for the NPSG were analyzed using images from Moderate Resolution Imaging Spectroradiometer (MODIS) obtained from the Ocean Biology Processing Group (http://oceancolor.nasa.gov). Data for a 25 × 25 km region surrounding Stn ALOHA were binned to generate the average and standard deviation at 8 day intervals (e.g., mean of days 1–8 over 2002–2012). Monthly composites were generated for the North Pacific. Anomaly time series were calculated by difference of 2012 data relative to spatial or temporal averages. Sea Surface Height Anomaly (SSHA) was assessed using animations of satellite altimetry covering 15–30°N, 148–170°W and produced from Archiving, Validation, and Interpretation of Satellite Oceanographic (AVISO) data.

3. Results

3.1. Hydrographic Conditions

During July–September 2012 hydrographic conditions in the upper water column (0–200 m) showed both the expected seasonal characteristics of the oligotrophic gyre ecosystem based on the 1989–2011 climatology at Stn ALOHA and evidence of high day-to-day variability (Figure 1). At the beginning of the field campaign, during 10–20 July, the mean near-surface (0–25 m) seawater temperature was 24.7 ± 0.1 [standard deviation (SD)] °C (Figure 1a). During the following 5 weeks from 20 July to 28 August the 0–25 m seawater temperature increased steadily to a maximum of 25.6°C and then subsequently decreased during the remainder of the campaign (Figures 1b–1e). For the overall period during July–September 2012, the near-surface (0–25 m) seawater temperature was 0.7–0.9°C lower than the respective monthly

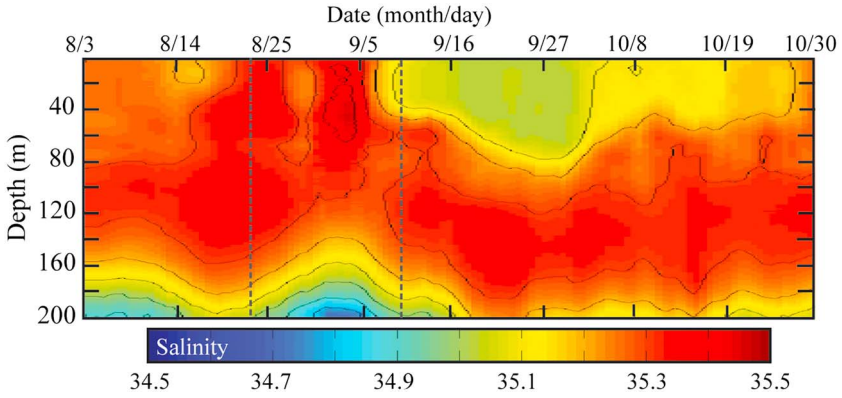

Figure 2. Upper water-column (0–200 m) profiles of salinity measured between 3 August and 30 October 2012 by a Seaglider. During September 2012, the Seaglider conducted 205 dives along ~370 km of the bowtie dive formation. The dashed lines indicate the time period when shipboard CTD profiles were conducted (shown in Figure 1).

averages from the 1989–2011 climatology at Stn ALOHA, reflecting a long-term interannual anomaly. The near-surface salinity ranged from 35.1 to 35.4 between July and mid-August 2012 (Figures 1f–1i). However, initially during 17–18 August and then more consistently from 26 August onwards, salinity decreased coincident with the passage of an upper ocean salinity minimum feature at Stn ALOHA. The mean salinity of the near-surface ocean during 17–18 August and from 6 September onwards was 35.0 which represented a mean decrease of 0.3 compared to the salinity measured during July 2012 (Figures 1f–1i). The feature was restricted to the near surface of the water column with salinity increasing to ~35.2 by a depth of 50 m. Dissolved O_2 concentrations in 0–25 m of the water column ranged from 209 to 218 μmol kg^{-1} (represented by the 5 and 95 percentile, respectively) with an overall mean of 212.0 ± 0.1 (SD) μmol kg^{-1} (Figures 1k–1o). Between depths of 50–100 m, a subsurface O_2 maximum was present with mean O_2 concentrations of 220 ± 3 (SD) μmol kg^{-1}. The deep chlorophyll maximum (DCM) was consistently present at depths between 100 and 150 m (Figures 1p–1t).

The mean MLD during 8–20 July 2012 was 66 ± 13 (SD) m, with a maximum depth of 86 m (Figure 1). For the remainder of the study period (20 July to 9 September) the MLD was shallower, with a mean depth of 51 ± 12 (SD) m. The prolonged period of deeper mixing in early July is unusual for the period of July–September at Stn ALOHA (the mean depth based on the 1988–2011 climatology is 49 ± 11 (SD) m). Shipboard observations at Stn ALOHA between 1989 and 2011 reveal five occurrences when the cruise-averaged-MLD exceeded 60 m during June–September based on a potential density anomaly of 0.125.

Satellite-derived SSHA in the ALOHA region between July and September 2012 suggested relatively modest eddy activity, with SSHA varying between −3.09 cm and 8.53 cm. The largest excursions in SSHA occurred in early July and September due to the westward advection of eddies approximately 180 km to the north of Stn ALOHA.

3.2. Sea-Surface Salinity Minimum at Stn ALOHA in August–September 2012

In addition to the shipboard CTD measurements (Figure 1), vertical profiles of salinity, temperature, and O_2 were collected by Seagliders (Figure 2) and Argo floats (Figure 3). These in situ observations provided an estimate of the temporal extent of the sea-surface salinity minimum feature observed in August–September (Figure 1j). The Seaglider traversed an area approximately 2500 km^2 in size, and the sea-surface salinity minimum feature was observed at Stn ALOHA until late September (0–25 m mean ± SD salinity of 35.1 ± 0.2), after which time salinity in the near-surface ocean returned to values more typical of late summer and early fall based on the HOT program climatology. Argo floats also detected the sea-surface salinity minimum both in September and prior to its arrival at Stn ALOHA in August (Figure 3). The sea-surface salinity minimum was most evident in the salinity profiles recorded by Argo float #5903888 (0–25 m depth-averaged salinity mean ± SD of 35.00 ± 0.03 during 12 September to 7 October), which profiled at 2 day intervals and was drifting clockwise around Stn ALOHA during July to December 2012 (Figure 3a). The two other Argo floats were located 200–300 km southeast of Stn ALOHA and recorded mean 0–25 m depth-averaged salinity of 35.0 ± 0.1 (SD) during 11 June and 25 September (Float #5903273; Figure 3b) and 35.0 ± 0.1 (SD) during 7 July and 25 September

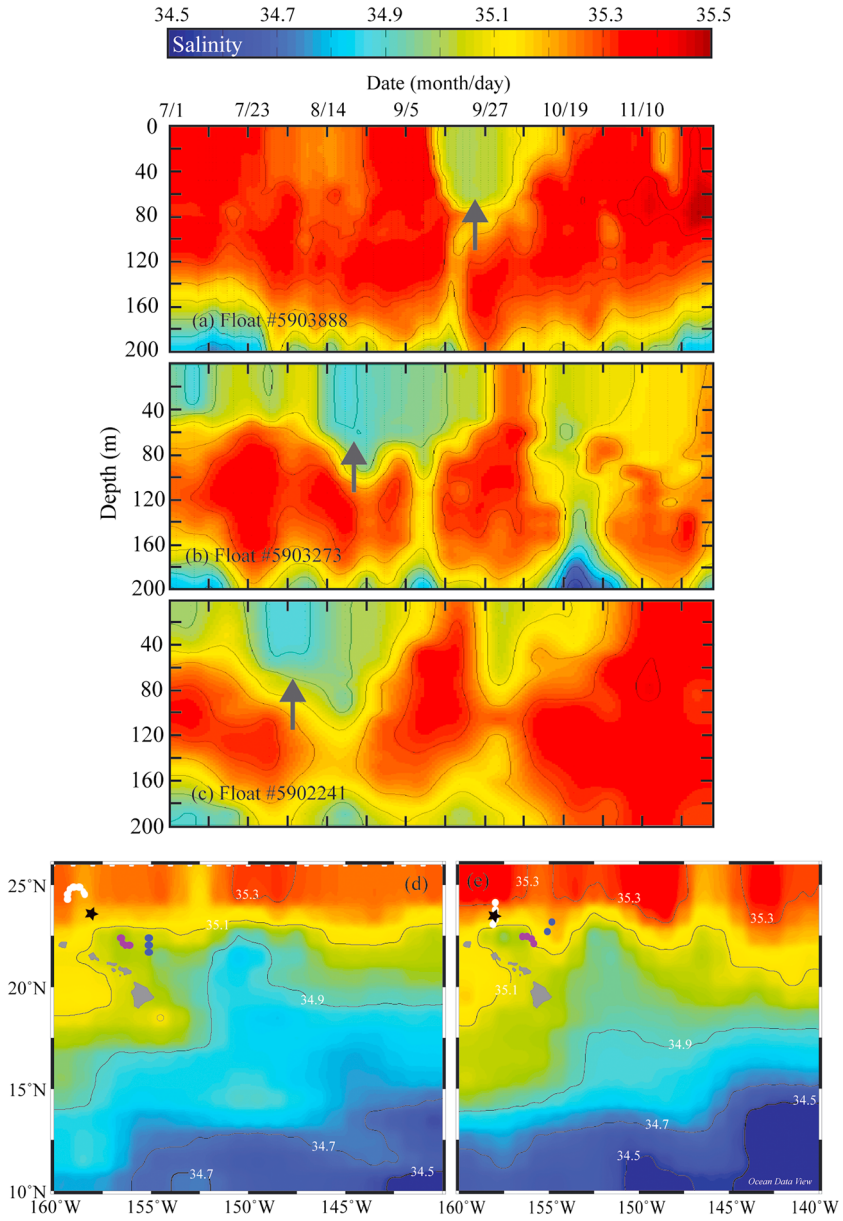

Figure 3. Figures 3a–3c are salinity profiles from three Argo floats in the vicinity of Stn ALOHA between July and November 2012 [*Roemmich and Gilson*, 2009]. The arrows represent surface salinity minimum features thought to correspond with the feature measured at Stn ALOHA in September 2012. Figures 3d and 3e are 0–100 m averaged salinity for August and September and include the position of the three Argo floats (#5903888 = white; #5903273 = purple, and #5902241 = blue) in relation to the Hawaiian Islands and Stn ALOHA (shown by a star).

(Float #5902241; Figure 3c). Similar to the Seagliders, the three Argo floats did not continue to detect the sea-surface salinity minimum in October, indicating that it had dissipated or propagated elsewhere undetected. Analysis of the Argo float data to the west and north of Stn ALOHA during September to December 2012 did not reveal any surface salinity minimum features. It is also noteworthy that neither the Argo floats nor the Seaglider detected the sea-surface salinity minimum on 17–18 August when it was sampled by the shipboard CTD, indicating the feature was initially irregular and hard to detect.

Efforts to determine the size and origin of the sea-surface salinity minimum proved difficult since it was not evident in satellite-derived measurements of salinity, and there were no changes in SSHA associated with the sea-surface salinity minimum. Analysis of circulation patterns generated by the HYCOM model revealed a mean sea-surface flow from the southeast during August to September 2012 (data not shown), and

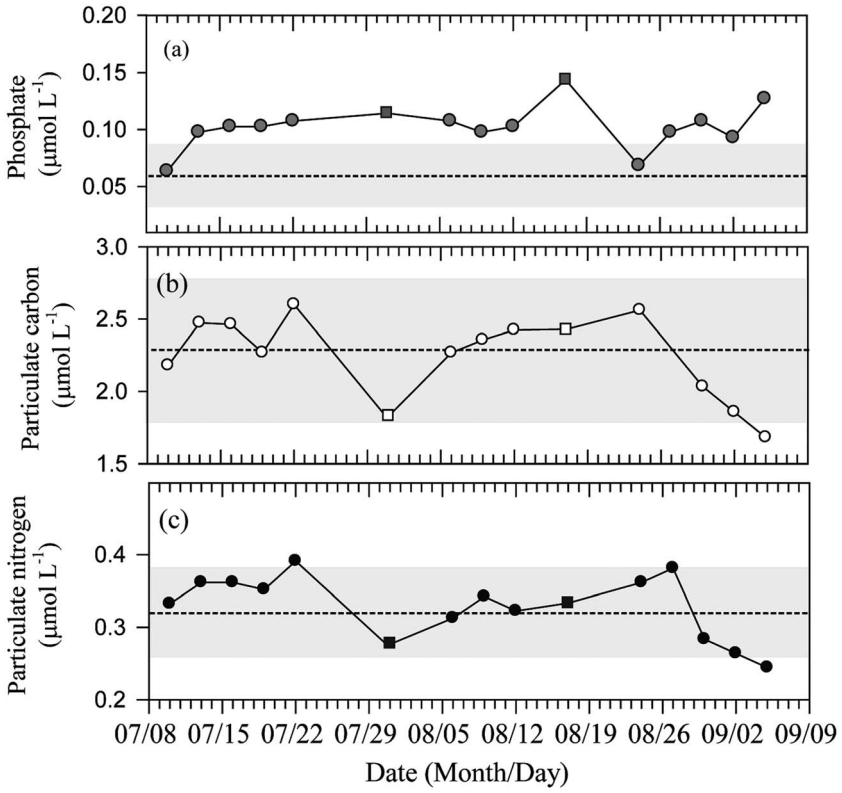

Figure 4. Depth-averaged (5–25 m) concentrations of (a) phosphate, (b) particulate carbon, and (c) particulate nitrogen during July–September 2012 at Stn ALOHA. The horizontal dashed line and shaded gray area represent the 5–25 m averaged mean concentration and standard deviation during 1989–2011 for the months of July–September. Measurements were made during C-MORE cruises (circles) and HOT cruises (squares).

Argo-derived salinity profiles indicated decreased near-surface salinity southeast of Stn ALOHA prior to September 2012 (Figures 3d and 3e). Using the Argo float monthly-averaged 0–100 m salinity during 2004–2014 for September, a northwest latitudinal shift of the mean salinity field by ~500 km would bring seawater with salinity of 35.0 to Stn ALOHA.

3.3. Water-Column Particulate Material and Nutrients

Water-column nutrients and particulate material were sampled at 3 day intervals or greater between depths of 0–175 m during July–September 2012. Depth-averaged (5–25 m) phosphate concentrations ranged from 0.07 to 0.14 μmol L^{-1} during July–September 2012 (Figure 4a). The phosphate concentrations during July–September are consistent with the 5–25 m depth-averaged values observed throughout 2012 (mean ± SD of 0.10 ± 0.02 μmol L^{-1}); however, the phosphate concentrations in 2012 are high compared to the overall mean of 0.06 ± 0.03 (SD) μmol L^{-1} for 1989–2011 climatological record. Hence, the elevated concentrations of phosphate in 2012 appear indicative of interannual variability, rather than short-term (monthly) variability. Concentrations of $NO_2^- + NO_3^-$ (not shown in Figure 4) were consistently low in the near-surface water column during July–September 2012. An increase in $NO_2^- + NO_3^-$ concentrations to 6–8 nmol L^{-1} (5–25 m depth-averaged) was recorded by the HOT program during July–August (http://hahana.soest.hawaii.edu/hot/hot-dogs) but not captured during the longer C-MORE expeditions which reported consistently low (2–5 nmol L^{-1}) concentrations.

During the period of study, the mean depth-averaged (5–25 m) concentration of PC was 2.3 ± 0.3 (SD) μmol L^{-1} (Figure 4b). The most distinct trend was observed during August–September as a persistent decrease in PC concentrations associated with the sea-surface salinity minimum. The lowest PC concentration of 1.70 ± 0.01 μmol L^{-1} was observed on 5 September. This is at the lower end of the long-term PC concentrations at Stn ALOHA for July–September, which range from 1.1 to 3.8 μmol L^{-1} (mean ± SD : 2.3 ± 0.5 μmol L^{-1}) based

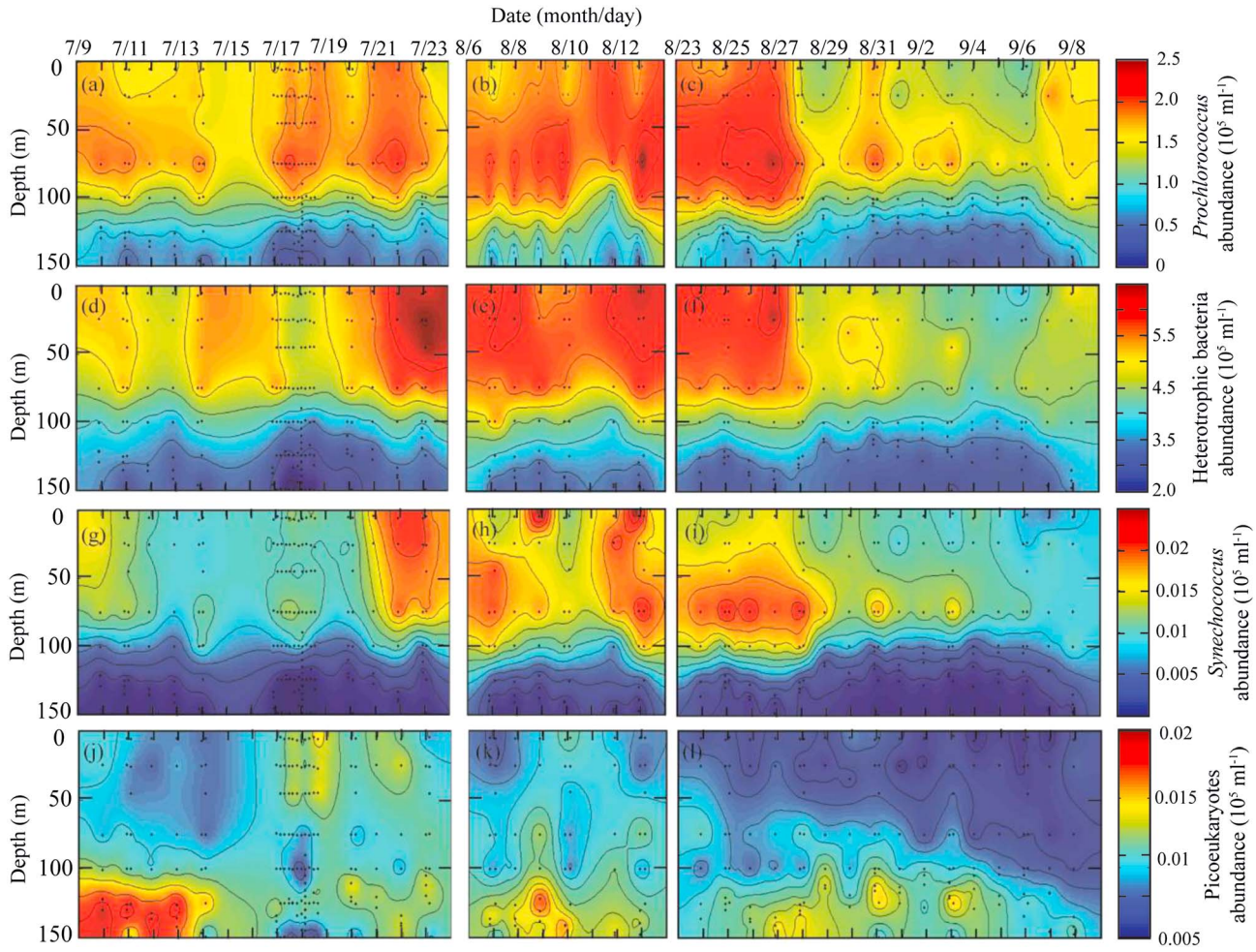

Figure 5. Depth profiles (0–150 m) of (a–c) *Prochlorococcus*, (d–f) heterotrophic bacteria, (g–i) *Synechococcus*, and (j–l) picoeukaryotes during July–September 2012 at Stn ALOHA.

on the 1989–2011 HOT climatology. In comparison, the mean 5–25 m depth-averaged concentration of PN for July–September was 0.32 ± 0.06 (SD) μmol L^{-1} (Figure 4c). A similar decreasing trend was observed in PN concentrations compared to PC toward the end of the campaign with the lowest PN concentration (0.24 μmol L^{-1}) measured on 5 September 2012 (Figure 4c).

3.4. Phytoplankton Community Composition

The abundance of flow cytometry-enumerated populations of phytoplankton and heterotrophic picoplankton (bacteria and archaea) in the upper water column showed a coherent and collective spatial and temporal pattern during July–September 2012 (Figure 5). The 5–25 m depth-averaged mean abundance of *Prochlorococcus* during the overall period from July to September was 1.6 ± 0.3 (SD) × 10^5 cells mL^{-1}. An approximate 17% decrease in 5–25 m depth-averaged mean cell abundance was observed during 1–7 September (1.4 ± 0.3 (mean ± SD) × 10^5 cells mL^{-1}), coincident with the presence of the sea-surface salinity minimum (Figures 5a–5c). Variability was also evident in the vertical distribution of *Prochlorococcus* with maximum cell abundances that occurred at 75 m where concentrations averaged 2.1 ± 0.3 (mean ± SD) × 10^5 cells mL^{-1} during July–September. The abundance of *Prochlorococcus* decreased rapidly with depth below 75 m, and cell concentrations were ~25% of the maximum abundance at 125 m. *Synechococcus* abundance at 5–25 m depths was 2 orders of magnitude lower than *Prochlorococcus* during July–September, with a mean abundance of 1.2 ± 0.4 (SD) × 10^3 cells mL^{-1} (Figure 5). Similar to the temporal patterns of *Prochlorococcus*, the population of *Synechococcus* also decreased during 1–7 September by

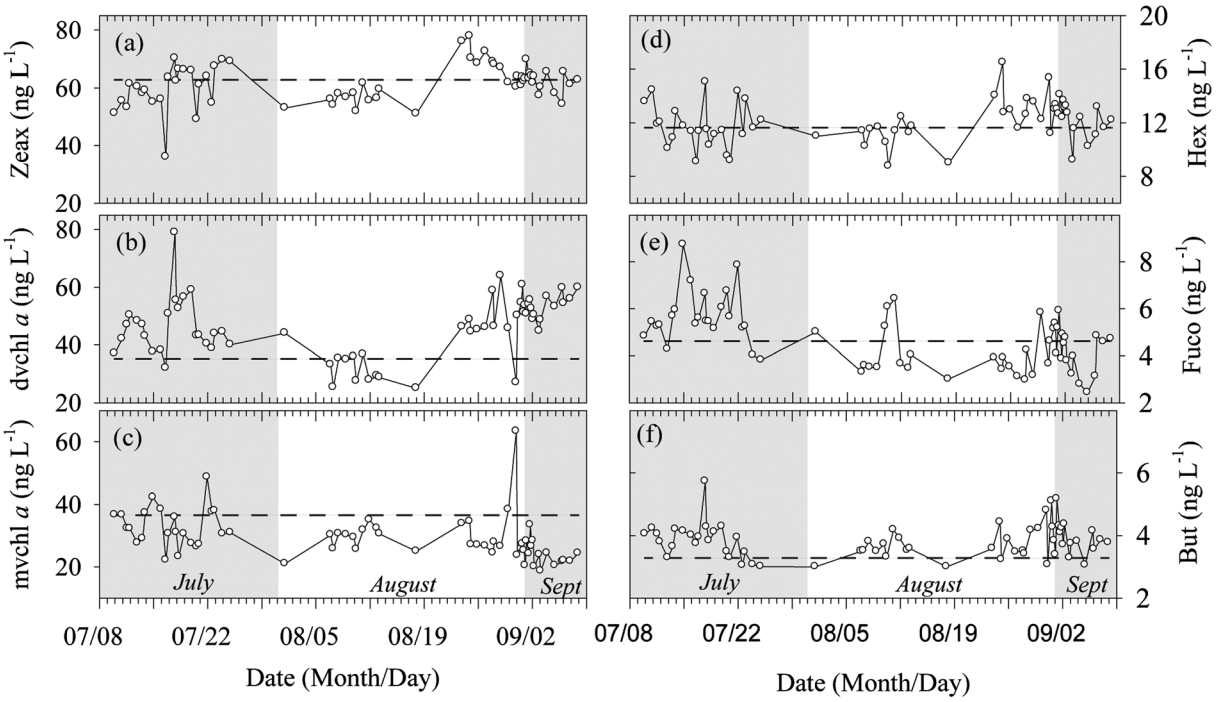

Figure 6. Temporal changes in depth-averaged (5–25 m) concentrations of diagnostic pigment biomarkers including HOT data: (a) zeaxanthin, (b) divinylchlorophyll *a*, (c) monovinylchlorophyll *a*, (d) 19′-hexanoyloxyfucoxanthin, (e) fucoxanthin, and (f) 19′-butanoyloxyfucoxanthin. The horizontal dashed line represents the mean concentration for each respective pigment averaged for July–September using the 1989–2011 HOT climatological record.

~28% with a mean cell abundance of 0.8 ± 0.1 (SD) $\times 10^3$ cells mL^{-1} (Figure 5). The mean abundance of photosynthetic picoeukaryotes between 5 and 25 m was 0.9 ± 0.3 (SD) $\times 10^3$ cells mL^{-1} during July–September (Figures 5j–5l), and the mean abundance of free-living heterotrophic picoplankton was 5.2 ± 0.7 (SD) $\times 10^5$ cells mL^{-1} (Figures 5d–5f). The effect of the sea-surface salinity minimum was also evident in populations of photosynthetic picoeukaryotes and heterotrophic picoplankton which were 33% and 24% less abundant between depths of 5–25 m during 1–7 September compared to July–August 2012.

In addition to flow cytometry enumerations of cell abundance, phytoplankton pigments at the 25 m depth horizon were sampled at daily (or more frequent) intervals, in addition to vertical profiles every 3 days (Figure 6). The most abundant pigments analyzed were zeaxanthin (Figure 6a), divinylchlorophyll *a* (Figure 6b), and monovinylchlorophyll *a* (Figure 6c). Divinylchlorophyll *a*, the diagnostic pigment for *Prochlorococcus*, was lower in concentration during 7–14 August with a mean concentration of 31 ± 4 (SD) ng L^{-1} compared to 7–23 July (mean ± SD: 46 ± 10 ng L^{-1}) and 23 August to 10 September (mean ± SD: 51 ± 7 ng L^{-1}) (Figure 6b). Daily excursions in pigment concentrations were occasionally observed (e.g., 31 August) and coincided with small-scale patterns in local hydrography (Figure 1). Of the three lesser abundant pigments, 19′-hexanoyloxyfucoxanthin and fucoxanthin, diagnostic biomarkers for prymnesiophytes and diatoms, respectively, displayed the largest variability during July–September 2012 (Figures 6d and 6e). The highest concentrations of fucoxanthin were observed in July (mean ± SD: 6 ± 1 ng L^{-1}) with concentrations subsequently decreasing steadily throughout the summer (Figure 6e).

Depth-averaged (5–25 m) concentrations of *nifH* gene copies for four major groups of N_2 fixing microorganisms are shown in Figure 7. UCYN-A was the most prominent diazotroph during July–September 2012 with an overall mean abundance of 6.8 ± 5.0 (SD) $\times 10^5$ *nifH* gene copies L^{-1}. *Trichodesmium* increased in abundance during the summer to reach a maximum gene abundance of 4.4×10^4 *nifH* gene copies L^{-1} during late August–September. The heterocystous cyanobacteria were most abundant in July with a mean concentration of 7.1 ± 1.5 (SD) $\times 10^3$ *nifH* gene copies L^{-1} and subsequently decreased in abundance during the summer. *Crocosphaera* was detected throughout July–September with a mean gene abundance of 6.4 ± 3.4 (SD) $\times 10^3$ *nifH* gene copies L^{-1}.

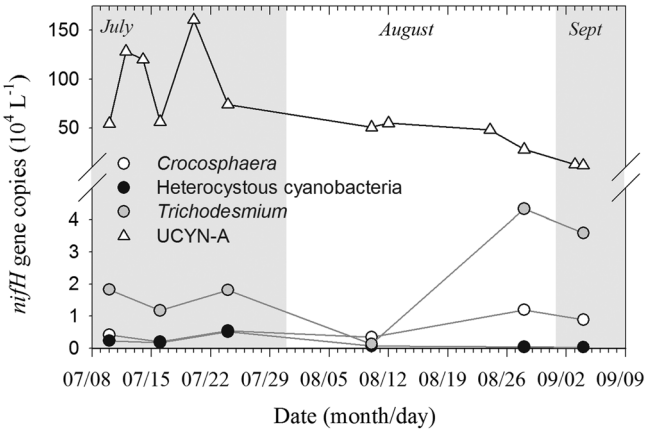

Figure 7. Depth-averaged (5–25 m) *nifH* gene copies during July–September 2012 for four major groups of diazotrophs: UCYN-A, *Crocosphaera*, heterocystous cyanobacteria, and *Trichodesmium*.

3.5. Productivity Measurements

Measurements of O_2/Ar ratios and ^{14}C assimilation were conducted during all three major expeditions, while FFRF and $^{17}\Delta$ were limited to fewer measurements (Figure 8 and Table 2). The O_2/Ar measurements are represented by ΔO_2/Ar (%) including the linear regressions used to calculate real-time O_2/Ar-NCP (Figure 8a) and prior O_2/Ar-NCP in units of mmol O_2 m^{-2} d^{-1} (Figure 8b). Rates of prior O_2/Ar-NCP were significantly different (*t*-test, $p < 0.01$) for each of the major expeditions and demonstrated a clear change between net autotrophic and net heterotrophic conditions in the near-surface waters (Figures 8a and 8b). During 9–24 July, the mean prior O_2/Ar-NCP was 6.0 ± 3.2 (SD) mmol O_2 m^{-2} d^{-1}, while the real-time O_2/Ar-NCP was 1.6 ± 2.6 (SD) mmol O_2 m^{-2} d^{-1}. The decrease in O_2/Ar-NCP during July ultimately led to net heterotrophic conditions being present in the mixed layer by the time daily measurements were resumed on 5 August. During 5–12 August, the mean MLD-integrated prior O_2/Ar-NCP was -7.6 ± 4.2 (SD) mmol O_2 m^{-2} d^{-1}, while real-time O_2/Ar-NCP was positive 3.9 ± 2.2 (SD) mmol O_2 m^{-2} d^{-1}, indicating the ecosystem had either recovered from the period of net heterotrophy or there was spatial variability in ΔO_2/Ar. While temporal trends on weekly timescales were present in rates of real-time O_2/Ar-NCP during 8–24 July and 5–12 August (Figure 8a), this was not the case for 22 August to 5 September (Figure 8a). In the absence of temporal trends of weekly timescales, O_2/Ar measurements during 23 August to 6 September were characterized by high day-to-day variability with a mean MLD-integrated prior O_2/Ar-NCP of -0.5 ± 3.1 (SD) mmol O_2 m^{-2} d^{-1}. The variability in prior O_2/Ar-NCP both preempted and coincided with the arrival of the sea-surface salinity minimum feature and therefore was likely due to high spatial variability.

Rates of ^{14}C-PP sampled at 25 m during every major expedition similarly revealed distinct patterns during July–September 2012 (Figure 8c). The highest rates of ^{14}C-PP occurred during 9–25 July with a mean of 0.61 ± 0.10 (SD) mmol C m^{-3} d^{-1} (MLD-integrated 36.3 ± 6.5 mmol C m^{-2} d^{-1}). The lowest rates occurred during 6–12 August with a mean value of 0.49 ± 0.1 (SD) mmol C m^{-3} d^{-1} (MLD-integrated 26.7 ± 5.1 mmol C m^{-2} d^{-1}). During 23 August to 8 September, the rates of ^{14}C assimilation ranged from 0.48 to 0.72 mg C m^{-3} d^{-1}, with an overall mean of 0.62 ± 0.1 (SD) mmol C m^3 d^{-1} (MLD-integrated 33.1 ± 7.4 mmol C m^{-2} d^{-1}). A comparison of the three expeditions revealed significantly lower rates of ^{14}C assimilation during 7–14 August (*t*-test, $p < 0.001$); however, there was no significant difference between the ^{14}C assimilation rates during 9–25 July and 23 August to 7 September (*t*-test, $p > 0.05$; Table 2).

The FRRF-based measurements of productivity (FRRF-PP) were conducted during 9–25 July and 23 August to 8 September (Figure 8d). There was no significant difference (*t*-test, $p > 0.05$) between the mean values of FRRF-PP measured at a depth of 25 m during the two expeditions which were 0.66 ± 0.13 (SD) mmol C m^{-3} d^{-1} for 9–25 July and 0.72 ± 0.07 (SD) mmol C m^{-3} d^{-1} for 23 August to 8 September. A consistent downward trend in FRRF-PP was observed during 23 August to 4 September which coincided with the decreasing concentrations of PC (Figure 4). The values of FRRF-PP are provided in Table 2 as MLD-integrated rates of production, using the MLD values provided in the supporting information.

Measurements of dissolved triple O_2 isotopes to determine GPP ($^{17}\Delta$-GPP) were conducted on 22 separate occasions during 23 August to 7 September (Table S2). The mean MLD-integrated $^{17}\Delta$-GPP for the 12 day period was 91 ± 35 (SD) mmol O_2 m^{-2} d^{-1} (range of 38–168 mmol O_2 m^{-2} d^{-1}). The analysis of duplicate seawater samples on the 28 August yielded a mean ± SD of 51 ± 5 mmol O_2 m^{-2} d^{-1} (Table S2). The $^{17}\Delta$-GPP was almost threefold higher than MLD-integrated ^{14}C-PP and 40% higher than MLD-integrated FRRF-PP during 23 August to 7 September (Table 2).

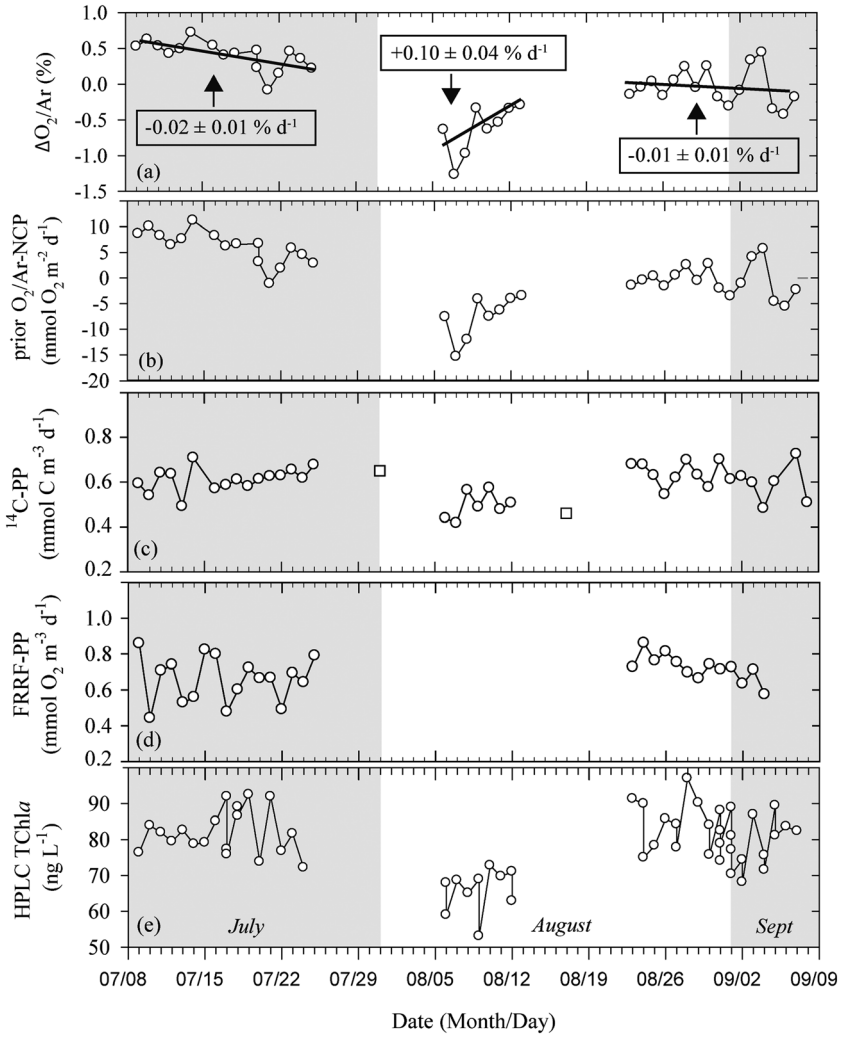

Figure 8. Productivity and TChl*a* (sum of monovinyl+divinylchlorophyll *a*) at Stn ALOHA from July through September 2012: (a) $\Delta O_2/Ar$ (%), (b) prior O_2/Ar-NCP, (c) ^{14}C-PP including HOT data as square symbols, (d) FRRF-PP, and (e) TChl*a*. The samples were collected at a depth of 25 m, and the gray shaded areas indicate months of year.

The significant period of low productivity when the upper water column was in a net heterotrophic state was explored using other data sets including phytoplankton biomarkers, time-series climatological measurements, and satellite-derived TChl*a*. During 7–12 August, the low rates of productivity coincided with low concentrations of TChl*a*, an indicator of photosynthetic biomass (Figure 8e). The mean concentration of TChl*a* decreased at the 25 m depth horizon from 82 ± 6 (SD) ng L^{-1} in 9–25 July by 30% to 66 ± 6 (SD) ng L^{-1} in 6–13 August (Figure 8e). The mean concentration of TChl*a* subsequently increased to an average concentration of 82 ± 7 (SD) ng L^{-1} for 23 August to 7 September (Figure 8e). A comparison of the three expeditions revealed significantly lower concentration of TChl*a* during 7–12 August (*t*-test, $p < 0.001$); however, there was no significance difference between concentration of TChl*a* during 9–25 July and 23 August to 7 September (*t*-test, $p > 0.05$).

The HOT program's near-monthly measurements at Stn ALOHA of ^{14}C assimilation and particle export rates during March–October 2012 are shown in comparison with the 1989–2011 HOT climatology (Figure 9). The monthly time-series measurements support the observation of low productivity occurring during August 2012. The mean depth-averaged (5–25 m) rates of ^{14}C-PP rates measured on 17 August was 0.44 mmol C m^3 d^{-1} (Figure 9a), equivalent to a MLD-integrated rate of ^{14}C-PP of 20.6 mmol C m^{-2} d^{-1}. These rates of ^{14}C-PP are low for this time of year at Stn ALOHA with a monthly mean for August based on the 1989–2011 HOT climatology of 0.66 ± 0.20 mmol C m^{-3} d^{-1} (Figure 9a). In addition to ^{14}C assimilation, during 17–18 August 2012, measured downward

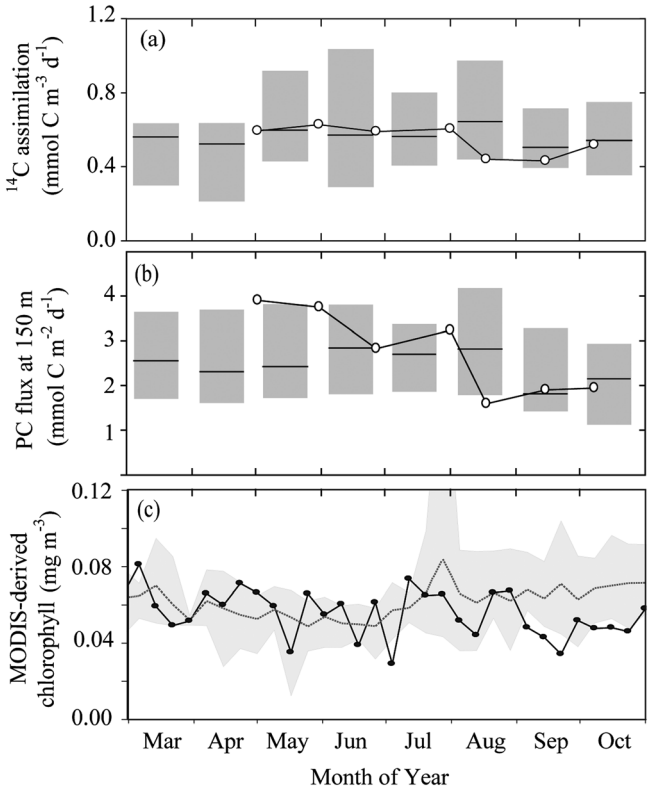

Figure 9. Comparison of key parameters in March–October 2012 with historical data. (a) ^{14}C-PP (5–25 m depth-averaged) and (b) particulate carbon flux measured at 150 m during March–October 2012 with 1989–2011 climatology. The values measured in 2012 are shown as white circles. The 1989–2011 data are binned by month and are shown as gray bars with the upper and lower boundaries represented by the 5 and 95 percentile and the mean value for each month shown by the horizontal black line. (c) Comparison of MODIS-derived chlorophyll *a* concentrations at Stn ALOHA in March–October 2012 with 2002–2014. The 2012 values are shown by a solid black line and closed circles, and the 2002–2014 values are represented by the dashed gray line (mean) and the shaded gray area (minimum and maximum).

export of C was 1.5 mmol C m^{-2} d^{-1}, almost half of the mean ± SD (2.9 ± 0.9 mmol C m^{-2} d^{-1}) for the month of August during the 1989–2011 Stn ALOHA climatology (Figure 9b).

The spatial and temporal extent for the period of low productivity was further investigated using remote sensing products provided by MODIS. Satellite-derived TChl*a* concentrations for 2012 are compared with the antecedent 10 year climatology (Figure 9c). The period of low productivity observed during 4–14 August by shipboard measurements is accompanied by a decrease in satellite-derived TChl*a* relative to the 10 year mean. However, there is a temporal mismatch with the shipboard measurements of TChl*a*, as determined by HPLC and fluorometry, as the satellite data show the largest TChl*a* anomaly to be in September 2012 when concentrations of TChl*a* are less than the minimum values observed in the 10 year climatology. In contrast, the shipboard observations show August to have the lowest TChl*a* concentrations (Figure 8e). A broader look at the TChl*a* anomaly throughout the NPSG reveals the negative anomaly is evident in August–September but not earlier in July 2012 (Figure 10). Albeit patchy, the negative TChl*a* anomaly during August–September extended from 22–26°N to 152–160°W, a region of approximately 300,000 km^2.

4. Discussion

4.1. Insights From High-Resolution Sampling in July–September 2012

The NPSG is a characteristic oligotrophic ecosystem with warm, stable conditions aided by strong seasonal stratification. Time-series observations conducted by the HOT program at Stn ALOHA for nearly three decades have characterized the frequently subtle seasonal and interannual variability associated with key physical and biological processes. For example, 0–200 m depth-integrated rates of primary productivity as determined by ^{14}C assimilation during 1988–2012 are 1.5 times higher in June–August (mean ± SD: 50.7 ± 11.8 mmol C m^{-2} d^{-1}) compared to December–February (mean ± SD: 34.7 ± 8.5 mmol C m^{-2} d^{-1}). One of the benefits of the long-term time-series observations is the ability to report the monthly or seasonal variability throughout several decades, and the mean rate of ^{14}C assimilation in the month of August is 52.6 ± 11.1 (SD) mmol C m^{-2} d^{-1}, ranging from 39.8 to 68.8 mmol C m^{-2} d^{-1} (represented by the 5 and 95 percentile values). This highlights that the variability within a single month can almost equal the variability measured within an entire annual period, suggesting that the short-term phenomena (e.g., phytoplankton blooms, mesoscale eddies, and wind-driven mixing) play an important role in shaping elemental cycling and phytoplankton growth. Until now however, high-resolution analysis of a single

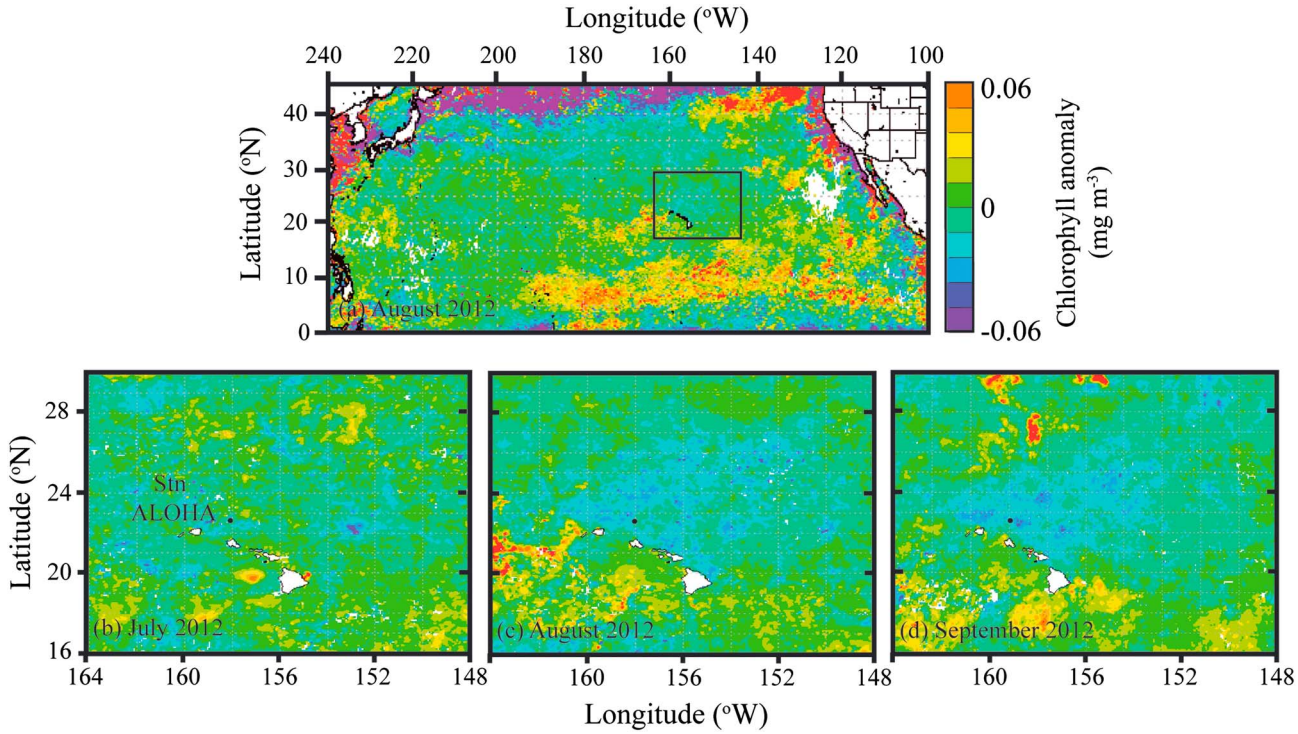

Figure 10. Anomaly of chlorophyll *a* concentration during August 2012 for (a) North Pacific Ocean and Stn ALOHA and the vicinity during (b) July, (c) August, and (d) September 2012. The box drawn around the Hawaiian Islands (Figure 10a) corresponds to the latitude and longitude shown in Figures 10b–10d.

seasonal period using intensive shipboard time-series measurements has not been conducted alongside the HOT program.

During July–September 2012, high temporal-resolution sampling at Stn ALOHA revealed changes in water-column biogeochemical properties over timescales of days to weeks. Overall, the measurements recorded a period of anomalously low productivity with a prolonged event of net heterotrophy in the upper water column. Our observations coincided with an absence of mesoscale eddies, a near-ubiquitous feature of the NPSG which advect through Stn ALOHA. While the focus of this study was on the upper ocean productivity and community composition (section 4.2), an analysis of the longer-term temporal variability and the wider NPSG is required to contextualize the findings from July to September 2012 (section 4.3).

4.2. Productivity and Community Structure in July–September 2012

An overall picture of NCP at Stn ALOHA between July and September 2012 is provided by the daily measurements of O_2/Ar ratio. Positive rates of NCP were initially measured in early July but began to decrease until ultimately net heterotrophic conditions were recorded in early August. It is unfortunate that the transition period occurred in-between the two expeditions although noteworthy that the changes occurred over timescales of several weeks. Overall, it is unusual for such a prolonged period of net heterotrophy to be present during the summer at Stn ALOHA [*Emerson et al.,* 1997; *Juranek and Quay*, 2005; *Quay et al.,* 2010]. The magnitude of the low productivity is apparent when comparing prior O_2/Ar-NCP measured during 6–12 August in units of O_2 (-7.6 ± 4.2 mmol O_2 m^{-2} d^{-1}) with the summary of NCP measurements previously reported for Stn ALOHA based on in situ geochemical methods (ranging from 3 to 11 mmol O_2 m^{-2} d^{-1}) [*Williams et al.,* 2013, and references therein]. The mixed layer community subsequently recovered from the period of net heterotrophy, although rates of NCP were still comparatively low during 22 August to 6 September which was attributed to the sea-surface salinity minimum. The three cruises are examined chronologically with regard to productivity and biological community composition.

During July, the mixed layer depth became progressively more shallow (Figure 1), and from 20 July onwards (for the next 5 weeks), the near-surface seawater (0–25 m) temperature increased by 1°C. During 7–23 July, $\Delta O_2/Ar$ values were at their maximum and recorded during July–September, and the mean MLD-integrated prior O_2/Ar-NCP was 6.0 ± 3.2 (SD) mmol O_2 m^{-2} d^{-1}. During this period, although the $\Delta O_2/Ar$ values were positive, indicating recent net autotrophic production, there was a decrease in $\Delta O_2/Ar$ values with time, indicating that either the system was not in steady state or there was some spatial variability in $\Delta O_2/Ar$. Estimated real-time O_2/Ar-NCP for this period was 1.6 ± 2.6 (SD) mmol O_2 m^{-2} d^{-1}, four times lower than the mean prior O_2/Ar-NCP. During this period, concentrations of fucoxanthin, the diagnostic pigment biomarker for diatoms, were at their summer maximum with a mean of 5.7 ± 1.1 (SD) ng L^{-1} (Figure 6e). Furthermore, the combined total *nifH* gene copies for heterocystous cyanobacteria were also at their maximum with an average abundance of 7.1 ± 1.5 (SD) $\times 10^3$ gene copies L^{-1} during 10–24 July (Figure 7). We therefore infer that the positive NCP during July was driven by diatoms that host symbiotic diazotroph assemblages. The identity of the heterocystous cyanobacteria determined by gene analysis was the endosymbiont *Richelia intracellularis* which is associated with the diatoms *Rhizosolenia* and *Hemiaulus* [*Foster and O'Mullan*, 2008]. High abundances of diatom-diazotroph assemblages have been associated with major increases in surface TChl*a* concentration [*Wilson*, 2003; *Fong et al.,* 2008; *Villareal et al.,* 2012], and the seasonal pulse of exported material that occurs at Stn ALOHA each year between July and August is thought to be fueled by these symbiotic microorganisms [*Karl et al.,* 2012]. A separate study on particle distributions in the euphotic zone at Stn ALOHA during July–September 2012 showed a positive correlation ($R^2 = 0.24$, $p < 0.05$) between fucoxanthin concentrations and 20–100 μm sized particles [*Barone et al.,* 2015]. Both fucoxanthin and 20–100 μm sized particles have the highest concentrations and the largest variability during July and are most likely the cause of the higher variability observed in the FRRF-derived estimates of productivity during July compared to the 22 August to 11 September expedition (Figure 8d).

By the start of the second leg of the three C-MORE expeditions (4–14 August), the pattern of NCP had changed. $\Delta O_2/Ar$ values were negative, indicating a recent period of net heterotrophy and prior O_2/Ar-NCP values were also negative with a mean value of -7.6 ± 4.2 mmol O_2 m^{-2} d^{-1}. However, $\Delta O_2/Ar$ values during this period showed an increase with time, and therefore, real-time O_2/Ar-NCP was positive, with a mean value of 3.9 ± 2.2 mmol O_2 m^{-2} d^{-1}. Again, this indicates that either the mixed layer was recovering from the period of net heterotrophy or there was spatial variability in $\Delta O_2/Ar$. The mismatch between prior and real-time NCP has been previously observed [*Hamme et al.,* 2012], whereas on other occasions, both approaches agree well [*Ferrón et al.,* 2015]. Rates of ^{14}C-PP were lowest during 6–12 August (mean ± SD: 26.7 ± 5.1 mmol C m^{-2} d^{-1}) and remained low until 18 August when in situ ^{14}C-PP measurements were conducted by the HOT program (Figure 9). The low productivity period was accompanied by a decrease in concentrations of photosynthetic pigments TChl*a* (Figure 8e), Zeax, and dvchl*a* (Figures 6a and 6b), indicating an accompanying shift in the dominant phytoplankton population. Despite changes in productivity and community composition, there was low variability in the hydrographic structure of the water column or nutrient conditions to accompany the rapid change from net autotrophic to net heterotrophic conditions. During 23 August to 7 September, measurements of ^{14}C-PP and O_2/Ar-NCP were accompanied by measurements of FRRF-PP and $^{17}\Delta$-GPP. Simultaneous measurements of the four methods of productivity are infrequently achieved, particularly for a 15 day period in the open ocean, and therefore offer an insight into the daily variability of these parameters when there was high spatial heterogeneity in the upper water column. While MLD-integrated prior O_2/Ar-NCP remained low for this period with a mean of -0.5 ± 3.1 (SD) mmol O_2 m^{-2} d^{-1}, rates of ^{14}C-PP had increased from the low values measured during 6–12 August to a mean of 33.1 ± 7.4 (SD) mmol C m^{-2} d^{-1}. Overall, MLD-integrated $^{17}\Delta$-GPP averaged 90.7 ± 35.3 mmol O_2 m^{-2} d^{-1} for the entire 15 day period and were comparable with previous measurements at Stn ALOHA in the summertime [*Juranek and Quay*, 2005; *Quay et al.,* 2010]. The high variability in the MLD-integrated $^{17}\Delta$-GPP measurements is supportive of the observation that there was high lateral heterogeneity in the surface seawater during this period. The O_2-based productivity estimates extrapolate for the residence time of O_2 in the mixed layer which sets a boundary on how much they can vary over a 24 h period. Considerable day-to-day variability was also observed in the O_2/Ar measurements with one of the largest decreases in prior O_2/Ar-NCP on 4 September when the near-surface water column became undersaturated (99.7%) in dissolved O_2 (Table S1). This coincided with a strong decrease in salinity associated with the sea-surface salinity minimum (Figure 1).

The most consistent temporal trend in the different measurements of productivity was evident in FRRF-derived estimates which decreased continually during the observation period. FRRF-PP is considered to more closely resemble GPP; however, it was ~40% lower than $^{17}\Delta$-GPP during 23 August to 7 September 2012. The decrease in FRRF-PP is coincident with decreasing concentrations of flow cytometry-enumerated phytoplankton abundance (Figure 5) and particulate material (Figure 4). Ultimately, the overall broad overview from this period is that the near-surface water column was recovering from a net heterotrophic state, although MLD-integrated prior O_2/Ar-NCP was still comparatively low and the sea-surface salinity minimum was accompanied by substantial spatial variability.

4.3. Further Analysis of the Low Productivity Period

It is unusual to observe an intensive period of net heterotrophic conditions during the summer at Stn ALOHA. The pronounced period of net heterotrophy occurred during the 4–14 August expedition; however, prior O_2/Ar-NCP during 26 August to 5 September was still relatively low (-0.5 ± 3.1 mmol O_2 m^{-2} d^{-1}) (Figure 8). Satellite observations revealed that the low productivity was not localized to Stn ALOHA, as an extensive low TChl*a* anomaly was evident from August through to September across the geographic area from 22–26°N to 152–160°W (Figure 10). The prolonged period of anomalous TChl*a* as revealed by MODIS (Figure 10) is somewhat contradictory to the shipboard pigment measurements (Figure 8e) where HPLC-derived TChl*a* increased in September relative to 4–14 August. However, it does suggest the low productivity was a regional phenomenon lasting for 1–2 months. In the absence of any local or regional physical forcing identified, wider ecosystem controls on productivity at Stn ALOHA are considered below.

One possible explanation for the low productivity is micro-nutrient limitation which would account for the build-up of phosphate that was at a higher concentration (0–100 m integrated values of 11.3 mmol m^{-2}) during 2012 than any other year (climatology ranges from 3.0 mmol m^{-2} in 2003 to 10.0 mmol m^{-2} in 1999) since 1988 (http://hahana.soest.hawaii.edu/hot/hot-dogs). The identification of the limiting micro-nutrient(s) was not investigated experimentally during this field program; however, near-surface concentrations of dissolved iron ranged from 0.14–0.87 nmol kg^{-1} (mean 0.31± 0.14 nmol kg^{-1}) throughout the summer and may have been limiting for certain phytoplankton species (Fitzsimmons et al., in revision *Geochimica et Cosmochimica Acta*). Another factor that directly influences growth and metabolism of marine plankton is seawater temperature [*Laws et al.,* 2000], which had a lower annual mean recording (24.5°C) between depths of 0 and 50 m during 2012 compared to the previous 12 years (24.6–25.4°C) (hahana.soest.hawaii.edu/hot/hot-dogs). However, the biogeochemical trends present in August 2012 should also be compared with longer timescales, and during the past 5 years (2009–2014), 0–100 m depth-integrated ^{14}C-PP has steadily increased (annual mean of 183 g C m^{-2} d^{-1} in 2009 compared to 233 g C m^{-2} d^{-1} in 2014), while the high phosphate concentrations observed in 2012 subsequently decreased and near-surface seawater temperatures subsequently increased (http://hahana.soest.hawaii.edu/hot/hot-dogs). An additional influence on productivity is near-surface water-column mixing. A "typical" mixed layer depth during the summertime at Stn ALOHA is 50 m, and during 2012, the upper water column did not stratify to this extent until late July. The ramifications of a delay in stratification on the diazotroph community which have been implicated in bloom formation in the NPSG [*Dore et al.,* 2008] are unclear, and their abundances during July–September (Figure 7) were at the lower end of their previously reported summertime abundances at Stn ALOHA [*Church et al.,* 2009]. Over longer-term timescales, a strengthening in stratification of the upper ocean is generally expected to cause decreased marine primary productivity in the subtropics, although this was not evident from historical analysis of the Stn ALOHA climatology [*Dave and Lozier*, 2010].

4.4. Sea-Surface Salinity Minimum

The hydrographic feature which has been described in this study was a sea-surface salinity minimum restricted to the upper water column and with biogeochemical properties distinct from the surrounding waters. Although it was difficult to track the source of the sea-surface salinity minimum with any certainty, ADCP and Argo float data indicate that it originated southeast of the Hawaiian Islands. This is supported by analysis of circulation patterns generated by the HYCOM model which revealed that the mean sea-surface flow was from the southeast during August to September 2012. The major ocean current to the southeast of the Hawaiian Islands is the North Equatorial Current, which extends from 10°N to 20°N

[*Bondur et al.,* 2008]. The North Equatorial Current bifurcates to the east of the island of Hawaii and the northern portion then contributes to the North Hawaii Ridge Current (NHRC), a weak predominantly westward flowing current [*Qiu et al.,* 1997; *Firing et al.,* 1999; *Bondur et al.,* 2008]. The magnitude of the NHRC varies considerably, ranging from undetectable to a maximum of 17 cm s^{-1} with no identified seasonal pattern in magnitude [*Firing*, 1996]. Its northern boundary is usually located south of Stn ALOHA, although it was detected intermittently at the time-series monitoring station [*Firing*, 1996].

The sea-surface salinity minimum described in this study provides an important example regarding the effect of discrete features (e.g., mesoscale eddy fields, meandering jets, and eddy dipoles) on biogeochemical variability at the ocean surface [*Williams and Follows,* 2011]. These features often have isolated water masses in their interiors for extended periods of time, indicative of transport barriers along their edges [*Harrison and Glatzmaier*, 2010]. For example, the transport of isolated water can provide nutrients into oligotrophic gyres which triggers biological productivity [e.g., *Bracco et al.,* 2000; *McGillicuddy et al.,* 2007]. In this instance, there was no evidence for nutrient injection into the oligotrophic ecosystem, and instead, the dominant effect of the isolation associated with sea-surface salinity minimum was a decline in biomass and productivity.

Ultimately, the community structure and biogeochemical signature associated with the sea-surface salinity minimum revealed a decreased microbial abundance which may have resulted from two factors. The first is that its properties are representative of the originating ecosystem remaining unchanged prior to its detection at Stn ALOHA. This is unlikely as a comparison of *Prochlorococcus*, *Synechococcus*, and heterotrophic bacteria abundance between Stn ALOHA and the tropical Pacific Ocean (0–10°N, 140°W) does not reveal major abundance differences [*Landry and Kirchman*, 2002]. The second explanation is that biological activity (death, cell lysis, and grazing) caused the decrease in biomass. The cumulative effects of these events would be quite significant (as is the case) due to the isolation of sea-surface salinity minimum from the surrounding water masses. In spite of the decrease in biomass an increase in inorganic nutrient concentrations which might be expected for net remineralization of the organic material was not observed. Most likely, the biological material was exported downwards with some retained at the base of the sea-surface salinity minimum (at depths of 50–70 m in the water column) due to the physical discontinuity resulting from strong stratification.

Although the in situ autonomous Seagliders and profiling floats were able to measure the extent of the sea-surface salinity minimum which continued through September (Figure 2), it is regrettable that the sampling of the feature was terminated at the end of the campaign. The decreasing concentrations of key water-column properties including particulate material, *Prochlorococcus* abundances, and prior O_2/Ar-NCP suggest that the full extent of the biogeochemical conditions associated with the sea-surface salinity minimum might not have been evaluated. Increasing deployment of in situ sensors to measure O_2 [*Riser and Johnson,* 2008], nutrients [*Johnson et al.,* 2010], and even community composition and activity [*Robidart et al.,* 2014] on autonomous vehicles will help attribute biogeochemical variability to discrete hydrographic features in the future.

5. Conclusion

In an oligotrophic gyre setting, where the ecosystem operates at the interface between net autotrophic to net heterotrophic conditions, our study shows that daily measurements are extremely informative when attempting to characterize intraseasonal variability and identify its drivers. In some instances, changes in plankton community could be related to episodic hydrographic features, e.g., decrease in cell abundance associated with the presence of the sea-surface salinity minimum. However, in other instances, such as the observed shift from net autotrophic to net heterotrophic conditions between July and August 2012, it is harder to explain the causes. Our inability to separate temporal from spatial variability through our Eulerian sampling approach highlights some of the difficulties faced in the study of pelagic microbial assemblages in which generation scales are in the order of days and kilometers. In the absence of local causation mechanisms being identified, larger spatial-temporal influences were investigated including nutrient concentrations, mixed layer depth, and seawater temperature. Ultimately, extensive ship operations lasting nearly 3 months are difficult to accomplish, and advances in obtaining sufficient spatial-temporal resolution will require the integration of autonomous, in situ instrumentation including floats, Seagliders, and moorings in collaboration with ship-based observations and experimentation.

Acknowledgments
The data set presented here resulted from the input of over 50 seagoing and shore-based oceanographers who contributed to the success of the field campaigns in 2012. We thank the Hawaii Ocean Time-series (HOT) program, the R/V *Kilo Moana* captain and crew, L. Fujieki for creating the C-MORE Data System which hosts the C-MORE field data (http://hahana.soest.hawaii.edu/cmoreDS/interface.html), S. Poulos for leading the Seaglider operations (http://hahana.soest.hawaii.edu/seagliders/), and P. Berube, T. Clemente, and S. Tozzi for cruise leadership. The WHOTS surface mooring data are provided by R.A. Weller and A.J. Plueddemann (http://www.soest.hawaii.edu/whots/) with funding from the NOAA Climate Observation Division. We thank H. Alexander, D. Böttjer, M. Segura-Noguera, and two anonymous reviewers for critical comments to the manuscript. This research was supported by the National Science Foundation (NSF) Center for Microbial Oceanography: Research and Education (C-MORE) (EF0424599 to D.M.K.), NSF grant OCE-1153656 (D.M.K), and a Gordon and Betty Moore Foundation Marine Microbiology Investigator award to D.M.K. The HOT program is supported by the NSF (OCE-1260164 to M.J.C, R.R.B., and D.M.K.).

References

Ascani, F., K. J. Richards, E. Firing, S. Grant, K. S. Johnson, Y. Jia, R. Lukas, and D. M. Karl (2013), Physical and biological controls of nitrate concentrations in the upper subtropical North Pacific Ocean, *Deep Sea Res., Part II*, *93*, 119–134, doi:10.1016/j.dsr2.2013.01.034.

Barone, B., R. R. Bidigare, M. J. Church, D. M. Karl, R. M. Letelier, and A. E. White (2015), Particle distributions and dynamics in the euphotic zone of the North Pacific Subtropical Gyre, *J. Geophys. Res. Oceans*, *120*, 3229–3247, doi:10.1002/2015JC010774.

Bidigare, R. R., L. Van Heukelem, and C. C. Trees (2005), Analysis of algal pigments by high-performance liquid chromatography, in *Algal Culturing Techniques*, edited by R. A. Andersen, pp. 327–345, Academic Press, New York.

Bidigare, R. R., F. Chai, M. R. Landry, R. Lukas, C. C. S. Hannides, S. J. Christensen, D. M. Karl, L. Shi, and Y. Chao (2009), Subtropical ocean ecosystem structure changes forced by North Pacific climate variations, *J. Plankton Res.*, *31*, 1131–1139, doi:10.1093/plankt/fbp064.

Bingham, F. M., and R. Lukas (1996), Seasonal cycles of temperature, salinity, and dissolved oxygen observed in the Hawaii Ocean time-series, *Deep Sea Res., Part II*, *43*, 199–213, doi:10.1016/0967-0645(95)00090-9.

Bondur, V. G., R. A. Ibrayev, Y. V. Grebenyuk, and G. A. Sarkisyan (2008), Modeling the sea currents in open basins: The case study for the Hawaiian Island region, *Izv. Atmos. Oceanic Phys.*, *44*, 225–235, doi:10.1134/S0001433808020102.

Bracco, A., A. Provenzale, and I. Sheuring (2000), Mesoscale vortices and the paradox of the plankton, *Proc. R. Soc. London, Ser. B*, *267*, 1795–1800, doi:10.1098/rspb.2000.1212.

Carritt, D. E., and J. H. Carpenter (1966), Comparison and evaluation of currently employed modifications of the Winkler method for determining dissolved oxygen in seawater; A NASCO report, *J. Mar. Res.*, *24*, 286–318.

Chassignet, E. P., et al. (2009), US GODAE: Global ocean prediction with the HYbrid Coordinate Ocean Model (HYCOM), *Oceanography*, *22*, 64–75, doi:10.5670/oceanog.2009.39.

Church, M. J., C. Mahaffey, R. M. Letelier, R. Lukas, J. P. Zehr, and D. M. Karl (2009), Physical forcing of nitrogen fixation and diazotroph community structure in the North Pacific subtropical gyre, *Global Biogeochem. Cycles*, *23*, GB2020, doi:10.1029/2008GB003418.

Church, M. J., M. W. Lomas, and F. Muller-Karger (2013), Sea change: Charting the course for biogeochemical ocean time-series research in a new millennium, *Deep Sea Res., Part II*, *93*, 2–15, doi:10.1016/j.dsr2.2013.01.035.

Corno, G., D. M. Karl, M. J. Church, R. M. Letelier, R. Lukas, R. R. Bidigare, and M. R. Abbott (2007), Impact of climate forcing on ecosystem processes in the North Pacific Subtropical Gyre, *J. Geophys. Res.*, *112*, C04021, doi:10.1029/2006JC003730.

Dave, A. C., and M. S. Lozier (2010), Local stratification control of marine productivity in the subtropical North Pacific, *J. Geophys. Res.*, *115*, C12032, doi:10.1029/2010JC006507.

Dore, J. E., and D. M. Karl (1996), Nitrite distributions and dynamics at Station ALOHA, *Deep Sea Res., Part II*, *43*, 385–402, doi:10.1016/0967-0645(95)00105-0.

Dore, J. E., R. M. Letelier, M. J. Church, R. Lukas, and D. M. Karl (2008), Summer phytoplankton blooms in the oligotrophic North Pacific Subtropical Gyre: Historical perspective and recent observations, *Prog. Oceanogr.*, *76*, 2–38, doi:10.1016/j.pocean.2007.10.002.

Dore, J. E., R. Lukas, D. W. Sadler, M. J. Church, and D. M. Karl (2009), Physical and biogeochemical modulation of ocean acidification in the central North Pacific, *Proc. Natl. Acad. Sci. U.S.A.*, *106*, 12,235–12,240, doi:10.1073/pnas.0906044106.

Duarte, C. M., A. Regaudie-de-Gioux, J. M. Arrieta, A. Delgado-Huertas, and S. Agustí (2013), The oligotrophic ocean is heterotrophic, *Annu. Rev. Mar. Sci.*, *5*, 551–569, doi:10.1146/annurev-marine-121211-172337.

Emerson, S. (2014), Annual net community production and the biological carbon flux in the ocean, *Global Biogeochem. Cycles*, *28*, 14–28, doi:10.1002/2013GB004680.

Emerson, S., P. Quay, D. Karl, C. Winn, L. Tupas, and M. Landry (1997), Experimental determination of the organic carbon flux from open-ocean surface waters, *Nature*, *389*, 951–954, doi:10.1038/40111.

Eriksen, C. C., T. J. Osse, R. D. Light, T. Wen, T. W. Lehman, P. L. Sabin, J. W. Ballard, and A. M. Chiodi (2001), Seaglider: A long-range autonomous underwater vehicle for oceanographic research, *IEEE J. Oceanic Eng.*, *26*, 424–436, doi:10.1109/48.972073.

Ferrón, S., S. T. Wilson, S. Martínez-García, P. D. Quay, and D. M. Karl (2015), Metabolic balance in the mixed layer of the oligotrophic North Pacific Ocean from diel changes in O_2/Ar saturation ratios, *Geophys. Res. Lett.*, *42*, 3421–3430, doi:10.1002/2015GL063555.

Firing, E. (1996), Currents observed north of Oahu during the first five years of HOT, *Deep Sea Res., Part II*, *43*, 281–303, doi:10.1016/0967-0645(95)00097-6.

Firing, E., B. Qiu, and W. Miao (1999), Time-dependent island rule and its application to the time-varying North Hawaiian Ridge Current, *J. Phys. Oceanogr.*, *29*, 2671–2688, doi:10.1175/1520-0485(1999)029<2671:TDIRAI>2.0.CO;2.

Fong, A. A., D. M. Karl, R. Lukas, R. M. Letelier, J. P. Zehr, and M. J. Church (2008), Nitrogen fixation in an anticyclonic eddy in the oligotrophic North Pacific Ocean, *ISME J.*, *2*, 663–676, doi:10.1038/ismej.2008.22.

Foster, R. A., and G. D. O'Mullan (2008), Nitrogen-fixing and nitrifying symbioses in the marine environment, in *Nitrogen in the Marine Environment*, edited by D. G. Capone et al., pp. 1197–1218, Elsevier Science, New York.

García, H. E., and L. I. Gordon (1992), Oxygen solubility in seawater: Better fitting equations, *Limnol. Oceanogr.*, *37*, 1307–1312, doi:10.4319/lo.1992.37.6.1307.

Goebel, N. L., K. A. Turk, K. M. Achilles, R. Paerl, I. Hewson, A. E. Morrison, J. P. Montoya, C. A. Edwards, and J. P. Zehr (2010), Abundance and distribution of major groups of diazotrophic cyanobacteria and their potential contribution to N_2 fixation in the tropical Atlantic Ocean, *Environ. Microbiol.*, *12*, 3272–3289, doi:10.1111/j.1462-2920.2010.02303.x.

Guidi, L., et al. (2012), Does eddy-eddy interaction control surface phytoplankton distribution and carbon export in the North Pacific Subtropical Gyre?, *J. Geophys. Res.*, *117*, G02024, doi:10.1029/2012JG001984.

Hamme, R. C., and S. R. Emerson (2004), The solubility of neon, nitrogen and argon in distilled water and seawater, *Deep Sea Res., Part I*, *51*, 1517–1528, doi:10.1016/j.dsr.2004.06.009.

Hamme, R. C., et al. (2012), Dissolved O_2/Ar and other methods reveal rapid changes in productivity during a Lagrangian experiment in the Southern Ocean, *J. Geophys. Res.*, *117*, C00F12, doi:10.1029/2011JC007046.

Harrison, C. S., and G. A. Glatzmaier (2010), Lagrangian coherent structures in the California Current System—Sensitivities and limitations, *Geophys. Astrophys. Fluid Dyn.*, *106*, 22–44, doi:10.1080/03091929.2010.532793.

Johnson, K. S., S. C. Riser, and D. M. Karl (2010), Nitrate supply from deep to near-surface waters of the North Pacific subtropical gyre, *Nature*, *465*, 1062–1065, doi:10.1038/nature09170.

Juranek, L. W., and P. D. Quay (2005), In vitro and in situ gross primary and net community production in the North Pacific Subtropical Gyre using labeled and natural abundance isotopes of dissolved O_2, *Global Biogeochem. Cycles*, *19*, GB3009, doi:10.1029/2004GB002384.

Kaiser, J., M. K. Reuer, B. Barnett, and M. L. Bender (2005), Marine productivity estimates from continuous O_2/Ar ratio measurements by membrane inlet mass spectrometry, *Geophys. Res. Lett.*, *32*, L19605, doi:10.1029/2005GL023459.

Kana, T. M., C. Darkangelo, M. D. Hunt, J. B. Oldham, G. E. Bennett, and J. C. Cornwell (1994), Membrane inlet mass spectrometer for rapid high-precision determination of N_2, O_2, and Ar in environmental water samples, *Anal. Chem.*, *66*, 4166–4170, doi:10.1021/ac00095a009.

Karl, D. M., and M. J. Church (2014), Microbial oceanography and the Hawaii Ocean Time-series programme, *Nat. Rev. Microbiol.*, *12*, 699–713, doi:10.1038/nrmicro3333.

Karl, D. M., and R. Lukas (1996), The Hawaii Ocean Time-series (HOT) program: Background, rationale and field implementation, *Deep Sea Res., Part II*, *43*, 129–156, doi:10.1016/0967-0645(96)00005-7.

Karl, D. M., R. R. Bidigare, and R. M. Letelier (2002), Sustained and aperiodic variability in organic matter production and phototrophic microbial community structure in the North Pacific subtropical gyre, in *Phytoplankton Productivity and Carbon Assimilation in Marine and Freshwater Ecosystems*, edited by P. J. Williams, D. R. Thomas, and C. S. Reynolds, pp. 222–264, Blackwell, Malden, Mass.

Karl, D. M., M. J. Church, R. M. Letelier, and C. Mahaffey (2012), Predictable and efficient carbon sequestration in the North Pacific Ocean supported by symbiotic nitrogen fixation, *Proc. Natl. Acad. Sci. U.S.A.*, *109*, 1842–1849, doi:10.1073/pnas.1120312109.

Keeling, C. D., H. Brix, and N. Gruber (2004), Seasonal and long-term dynamics of the upper ocean carbon cycle at Station ALOHA near Hawaii, *Global Biogeochem. Cycles*, *18*, GB4006, doi:10.1029/2004GB002227.

Kolber, Z., and P. G. Falkowski (1993), Use of active fluorescence to estimate phytoplankton photosynthesis *in situ*, *Limnol. Oceanogr.*, *38*, 1646–1665, doi:10.4319/lo.1993.38.8.1646.

Landry, M. R., and D. L. Kirchman (2002), Microbial community structure and variability in the tropical Pacific, *Deep Sea Res., Part II*, *49*, 2669–2693, doi:10.1016/S0967-0645(02)00053-X.

Laws, E. A. (1991), Photosynthetic quotients, new production and net community production in the open ocean, *Deep Sea Res., Part I*, *38*, 143–167, doi:10.1016/0198-0149(91)90059-O.

Laws, E. A., P. G. Falkowski, W. O. Smith Jr., H. Ducklow, and J. J. McCarthy (2000), Temperature effects on export production in the open ocean, *Global Biogeochem. Cycles*, *14*(4), 1231–1246, doi:10.1029/1999GB001229.

Letelier, R. M., J. E. Dore, C. D. Winn, and D. M. Karl (1996), Seasonal and interannual variations in photosynthetic carbon assimilation at Station ALOHA, *Deep Sea Res., Part II*, *43*, 467–490, doi:10.1016/0967-0645(96)00006-9.

Luz, B., and E. Barkan (2000), Assessment of oceanic productivity with the triple-isotope composition of dissolved oxygen, *Science*, *288*, 2028–2031, doi:10.1126/science.288.5473.2028.

Martin, A. P. (2003), Phytoplankton patchiness: The role of lateral stirring and mixing, *Prog. Oceanogr.*, *57*, 125–174, doi:10.1016/S0079-6611(03)00085-5.

McGillicuddy, D. (2001), The internal weather of the sea and its influences on ocean biogeochemistry, *Oceanography*, *14*, 78–92, doi:10.5670/oceanog.2001.09.

McGillicuddy, D. J., Jr., et al. (2007), Eddy/wind interactions stimulate extraordinary mid-ocean plankton blooms, *Science*, *316*, 1021–1026, doi:10.1126/science.1136256.

Moisander, P. H., R. A. Beinart, M. Voss, and J. P. Zehr (2008), Diversity and abundance of diazotrophic microorganisms in the South China Sea during intermonsoon, *ISME J.*, *2*, 954–967, doi:10.1038/ismej.2008.51.

Qiu, B., D. A. Koh, C. Lumpkin, and P. Flament (1997), Existence and formation mechanism of the North Hawaiian Ridge current, *J. Phys. Oceanogr.*, *27*, 431–444, doi:10.1175/1520-0485(1997)027<0431:EAFMOT>2.0.CO;2.

Quay, P. D., C. Peacock, K. Björkman, and D. M. Karl (2010), Measuring primary production rates in the ocean: Enigmatic results between incubation and non-incubation methods at Station ALOHA, *Global Biogeochem. Cycles*, *24*, GB3014, doi:10.1029/2009GB003665.

Reuer, M. K., B. A. Barnett, M. L. Bender, P. G. Falkowski, and M. B. Hendricks (2007), New estimates of Southern Ocean biological production rates from O_2/Ar ratios and the triple isotope composition of O_2, *Deep Sea Res., Part I*, *54*(6), 951–974, doi:10.1016/j.dsr.2007.02.007.

Riser, S. C., and K. S. Johnson (2008), Net production of oxygen in the subtropical oceans, *Nature*, *451*, 323–325, doi:10.1038/nature06441.

Robidart, J. C., et al. (2014), Ecogenomic sensor reveals controls on N_2-fixing microorganisms in the North Pacific Ocean, *ISME J.*, *8*, 1175–1185, doi:10.1038/ismej.2013.244.

Roemmich, D., and J. Gilson (2009), The 2004–2008 mean and annual cycle of temperature, salinity, and steric height in the global ocean from the Argo Program, *Prog. Oceanogr.*, *82*, 81–100, doi:10.1016/j.pocean.2009.03.004.

Strickland, J. D. H., and T. R. Parsons (1972), *A Practical Handbook of Seawater Analysis*, 2nd ed., Fish. Res. Board of Can., Ottawa.

Suggett, D. J., K. Oxborough, N. R. Baker, H. L. MacIntyre, T. M. Kana, and R. J. Geider (2003), Fast repetition rate and pulse amplitude modulation chlorophyll a fluorescence measurements for assessment of photosynthetic electron transport in marine phytoplankton, *Eur. J. Phycol.*, *38*, 371–384, doi:10.1080/09670260310001612655.

Tortell, P. D., E. C. Asher, H. W. Ducklow, J. A. L. Goldman, J. W. H. Dacey, J. J. Grzymski, J. N. Young, S. A. Kranz, K. S. Bernard, and F. M. M. Morel (2014), Metabolic balance of coastal Antarctic waters revealed by autonomous pCO_2 and O_2/Ar measurements, *Geophys. Res. Lett.*, *41*, 6803–6810, doi:10.1002/2014GL061266.

Venrick, E. L. (1995), Scales of variability in a stable environment: Phytoplankton in the central North Pacific, in *Ecological Time Series*, edited by T. M. Powell and J. H. Steele, pp. 150–180, Chapman and Hall, New York.

Villareal, T. A., C. G. Brown, M. A. Brzezinski, J. W. Krause, and C. Wilson (2012), Summer diatom blooms in the North Pacific Subtropical Gyre: 2008–2009, *PLoS One, 7*(4), e33109, doi:10.1371/journal.pone.0033109.

Wanninkhof, R. (2014), Relationship between wind speed and gas exchange over the ocean revisited, *Limnol. Oceanogr. Methods*, *12*, 351–362, doi:10.4319/lom.2014.12.351.

Williams, P. J. B., P. D. Quay, T. K. Westberry, and M. J. Behrenfeld (2013), The oligotrophic ocean is autotrophic, *Annu. Rev. Mar. Sci.*, *5*, 535–549, doi:10.1146/annurev-marine-121211-172335.

Williams, R. G., and M. J. Follows (2011), *Ocean Dynamics and the Carbon Cycle: Principles and Mechanisms*, 404 pp., Cambridge Univ. Press, Cambridge, U. K.

Wilson, C. (2003), Late summer chlorophyll blooms in the oligotrophic North Pacific Subtropical Gyre, *Geophys. Res. Lett., 30*(18), 1942, doi:10.1029/2003GL017770.

Wilson, C., T. A. Villareal, M. A. Brzezinski, J. W. Krause, and A. Y. Shcherbina (2013), Chlorophyll bloom development and the subtropical front in the North Pacific, *J. Geophys. Res. Oceans*, *118*, 1473–1488, doi:10.1002/jgrc.20143.